STUDY OF THE ELECTRONIC SURFACE STATES OF III-V COMPOUNDS

Semi-Annual Technical Progress Report

1 October 1979 — 31 March 1980

Principal Investigators:

W. E. Spicer
I. Lindau

Telephone: 415 497-4643

Office of Naval Research
Department of the Navy
Arlington, Virginia 22217

Sponsored by

DEFENSE ADVANCED RESEARCH PROJECTS AGENCY
DARPA Order No. 3564
Program Code No. HX1241

Contract No. N00014-79-C-0072
DARPA Order No. 3564

Effective: 1 October 1979 Expiration: 30 September 1980 ($181,890)

Stanford Electronics Laboratories
Stanford University
Stanford, California 94305

CONTENTS

		Page
I.	OVERVIEW	1
II.	SUMMARY OF APPENDED PAPERS	2
	A. The Unified Defect Model	2
	B. Column III and V Elements on GaAs (110)	2
	C. Oxygen on GaAs (110)	3
	D. Metal-Si Interfaces	4
III.	SUMMARY OF MOST RECENT RESULTS	6
IV.	ARTICLES PUBLISHED DURING PERIOD	7

Chapter I

OVERVIEW

At the time of the last semiannual report, we had stated the development of the unified defect model for Schottky-barrier formation. Since then, work has proceeded to further explain the nature and the source of states at the oxide:III-V interface and metal semiconductor interface. This is of crucial importance to the MOS technology. Along with the extension in scope of the unified defect model, more work to establish the model on a more refined and definitive basis has been carried out.

Making use of the techniques we have developed, we started studying on an atomic scale the bonding trends of column III and V elements on GaAs. This work is not only important to the understanding of the metal-semiconductor interface but also has very significant bearing on the crystal growth mechanism. For oxygen adsorption, we have studied in detail both the nature of Fermi-level pinning at very low oxygen coverage and surface chemistry near monolayer coverage. Work on metal-Si interaction has also been greatly advanced in the past six months. Analysis of prior results of Au on Si has been completed. Experiments of Pd on Si have been conducted and results have been analyzed.

Other activities during this period included the following.

(1) Completion of the construction of the treatment chamber. Efforts are now aiming at successfully controlling the As treatment of GaAs surfaces.

(2) Design, construction, and test of a miniature electron-beam evaporator. Installation of this evaporator in the treatment chamber allows clean deposition of many of the technologically important high-melting-point metals. This will immeasurably enlarge the scope of ou study of the metal-semiconductor system.

(3) Investigation of the optimum conditions and the availability of lasers for future laser-semiconductor interaction experiments.

Chapter II

SUMMARY OF APPENDED PAPERS

The appended papers represent the analyzed part of our experimental work in the past six months. In this chapter, we present a summary of the significance, results, and conclusions of each paper.

A. The Unified Defect Model

The unified defect model has been successful in explaining a wide variety of results as oxygen or a metal is added to the III-V surface. These results range from those involving a small fraction of a monolayer of adatoms to practical III-V structures with very thick overlayers. The tenets of this model are outlined, and the experimental results leading to its formulation are briefly reviewed. InP levels 0.4 and 0.1 eV and GaAs levels 0.7 and 0.9 eV below the conduction-band minimum (CBM) are associated with either missing column III or V elements. In InP, it has been found possible by a number of workers to "switch" between the two defect levels by variations in surface processing, temperature, and/or selection of the deposited atom. The need to apply the proper concepts for surface and interface chemistry and metallurgy is recognized, and the danger of using solely bulk concepts is emphasized. The reason for this is examined for certain cases on an atomic level. The need for new fundamental attacks on interface interactions is recognized and emphasized. The importance of semiconductor-oxide chemical stability is also recognized and, drawing on a large body of work from several laboratories, it is suggested that there will be more difficulties with "native" oxides on GaAs than on InP. An attempt is made to give an overview with the conclusion that "scientific engineering" of interfaces to give optimum performance should be a goal and test of the fundamental work. Specific possibilities are discussed for Schottky barriers on III-V's.

B. Column III and V Elements on GaAs (110)

The nature of adatom bonding onto semiconductor sufaces is of considerable practical importance. Passivation, contacts (Schottky or

ohmic), and control of the growth mode of the crystal may all depend on the nature of such bonding. This appendix is directly related to the growth of III-V crystals since we are depositing elements which are isoelectronic with the semiconductor components--column III and V elements. Our results can be most easily applied to crystal growth by molecular beam epitaxy (MBE) since our experimental conditions and techniques for depositing the adatoms onto a clean semiconductor surface are the same as those used for MBE. However, it should be noted that our results also have a strong impact on the understanding of metal-semiconductor bonding. Recently, there has been strong interest, both theoretical and experimental, in the bonding of column III metals on GaAs (110) as a model system for studying metal semiconductor bonding. In this appendix, we show that the bonding of these metal overlayers is fundamentally different and more complex than models proposed by other workers.

Our immediate goals are to identify the bond type and adatom bonding site for column III and V elements on GaAs (110). We have made very good progress on identifying the bond type (see appendix) but less progress in identifying the adatom site. Further experimental work on the metal overlayers is under way, and contact has been made with theorists in this field to enhance our interpretation of our results. Our results are already sufficient to suggest experiments in III-V crystal growth to test our models of the overlayers. In particular, we have proposed that it is the adsorbed column V element which forms the directional bond to the crystal with the adsorbed column III atoms anchoring themselves via covalent bonds to the adsorbed column V elements but not to the clean (110) face. By varying growth conditions, this model can be tested. Use of the preparation chamber, which has been described in previous reports and proposals, will greatly aid this study.

C. Oxygen on GaAs (110)

Work on the initial oxidation of GaAs (110)surfaces in this reporting period has emphasized two aspects:

(1) Understanding of the Fermi-level movement induced by oxygen adsorbed in very low coverage; this aspect of the work has its implication in the more general problem of

unified Fermi-level pinning theory of the semiconductor discussed earlier in this report.

(2) Understanding of the chemistry of oxygen adsorption near monolayer coverage; fundamental surface chemistry as determined from this part of the work has its implication in understanding and/or controlling the chemical properties of oxide/GaAs interfaces, which is an important issue confronting real device fabrication.

Major progress related to the first aspect of this work is the identification of two different forms of adsorbed oxygen through detailed analysis of the oxygen-induced structure in the valence-band region. Adsorption in the first form saturates at very low coverage (<0.01 monolayer) and is probably associated with cleavage steps. Detailed correlation of this first form to the Fermi-level movement is not yet available. However, the Fermi level is known to proceed toward stabilization at the same coverage where adsorption in the first form approaches saturation. Hence, the possible role of the first form of oxygen in inducing changes of the surface electronic structure cannot be overlooked. Of particular significance is the detection of the very low concentration of oxygen. Such high sensitivity allows quantitative assessment of defect (probably cleavage steps) sites through measurement of the saturation point of this form of adsorbed oxygen. This problem will be pursued in the future.

Adsorption in the second form occurs at normal surface sites and is related to the second aspect of this work. We have reported earlier the chemical shifts in Ga-3d and As-3d produced by the adsorption of the second form of oxygen and the difficulties associated with the interpretations of these shifts. We have demonstrated that, by heating surfaces adsorbed with oxygen at room temperature, such difficulties can be greatly reduced. A new picture of the surface chemistry of oxygen adsorption has thus emerged from our work.

D. Metal-Si Interfaces

Photoemission (PS) and Auger electron spectroscopy were used to study the formation of Pd silicide in UHV on Si single crystals. The Pd depositions ranged from submonolayer coverages to hundreds of Angstroms

thickness. AES sputter-depth profiles indicate that room-temperature Pd-Si interdiffusion occurs over ~1100 Å and that Pd reduces the native Si oxides, with oxygen appearing at the vacuum surface of the evaporated layer. We have been able to separate out the relative contributions of Si and Pd to the silicide valence band by using a wide range of photon energies in the PS studies. The Pd d-bands in the silicide are filled and, due to the strong Pd-Si interaction, are pulled down more than 2 eV relative to Pd metal. In addition, we suggest that the silicide formed at the surface may be more closely related to that of the glassy metals rather than the well-defined (although closely related) Pd_2Si compound. Similar results are also obtained for the system of Pt on Si.

Chapter III

SUMMARY OF MOST RECENT RESULTS

A number of new experiments are in progress and results are being analyzed. A brief summary of these preliminary results are given below.

Angle-resolved photoemission measurements of column III and V elements on GaAs (110) have been attempted with our current experimental setup. Even with the crude angle resolution and angle reproducibility of the current experimental system, we were able to obtain information which is inaccenssible to angle-integrated photoemission measurements. For example, features due to the dangling bond and back bonds of the surface atoms are well resolved and the changes induced by the metal-GaAs bonding are easily followed. These results well justify the needs for a refined angle-resolved photoemission measurement system. The experience gained here will serve as guidance to our future plan of purchasing an angle-resolved measurement system.

New studies of oxygen adsorption on the Si (111) 2 × 1 (cleaved) and Si (111) 7 × 7 (thermally converted from the cleaved) surfaces have produced important results. Substantial difference was found in both the oxygen sticking coefficient and the Si-O bonding configuration for the two surfaces. In all of the previously proposed models of oxygen adsorption on Si (111) surfaces, no distinction was made between the two differently reconstructed surfaces. Hence, this finding will have a definite impact on the understanding of the interaction of oxygen with Si as well as give insight into the nature of the two reconstructions.

As a first step in our test of the treatment chamber and the As evaporation source, we have successfully deposited a clean As film and obtained its UPS spectra. Oxidation properties of this film has also been studied. Results from this experiment will serve as a useful reference to future experiments of treating GaAs surfaces with As and oxidation of such surfaces.

Chapter IV

ARTICLES PUBLISHED DURING PERIOD

1. Photoemission Studies of the Initial Stages of Oxidation of GaSb and InP, P. W. Chye, C. Y. Su, I. Lindau, C. M. Garner, P. Pianetta, and W. E. Spicer, Surf. Sci. 88 (1979), pp. 439-460.

2. Studies of the Effect of Oxidation Time and Temperature on the $SiSiO_2$ Interface using Auger Sputter Profiling, C. R. Helms, N. M. Johnson, S. A. Scharz, and W. E. Spicer, J. Appl. Phys. 50, 11 (1979), pp. 7007-7014.

3. Oxidation of Ordered and Disordered GaAs (110), P. W. Chye, C. Y. Su, I. Lindau, Perry Skeath, and W. E. Spicer, J. Vac. Sci. Technol. 16, 5 (Sep-Oct 1979), p. 1191.

4. Investigation of the Mechanism for Schottky Barrier Formation by Group 3 Metals on GaAs, P. Skeath, I. Lindau, P. W. Chye, C. Y. Su, and W. E. Spicer, J. Vac. Sci. Technol. 16, 5 (Sep-Oct 1979), p. 1143.

5. Comparative Studies of Oxygen Adsorption on GaAs (110) Surfaces with Ultrathin Aluminum and Cesium Overlayers, Perry Skeath, C. Y. Su, P. W. Chye, P. Pianetta, I. Lindau, and W. E. Spicer, J. Vac. Sci. Technol. 16, 5 (Sep-Oct 1979), p. 1439.

6. Photoemission Studies of the Silicon-Gold Interface, L. Braicovich, C. M. Garner, P. R. Skeath, C. Y. Su, P. W. Chye, I. Lindau, and W. E. Spicer, Phys. Rev. B 20, 12 (Dec 1979), pp. 5131-5141.

7. Unified Mechanism for Schottky-Barrier Formation and III-V Oxide Interface States, W. E. Spicer, I. Lindau, P. Skeath, S. Y. Su, and Patrick Chye, Phys. Rev. Letts. 44, 6 (Feb 1980), pp. 420-423.

8. Use of Photoemission and Related Techniques to Study Device Fabrication, W. E. Spicer, Nondestructive Evaluation of Semiconductor Materials and Devices (Jay N. Zemel, ed.), Plenum Publishing Corp., 1979, Chapter 8.

9. Nature of Interface States at III-V Insulator Interfaces, W. E. Spicer, P. W. Chye, P. R. Skeath, C. Y. Su, and I. Lindau, Inst. Phys. Conf. Ser. No. 50 (1980), Chapter 4, pp. 216-233.

10. New and Unified Model for Schottky Barrier and III-V Insulator Interface States Formation, W. E. Spicer, P. W. Chye, P. R. Skeath, C. Y. Su, and I. Lindau, J. Vac. Sci. Technol. 16, 5 (Sep-Oct 1979), p. 1422.

APPENDIX A

In Press - J. Vac. Sci. and Tech. Oct./Nov. 1981

THE UNIFIED DEFECT MODEL AND BEYOND

W. E. Spicer,* I. Lindau,
P. Skeath, and C. Y. Su
Electrical Engineering Department
Stanford University
Stanford, California 94305

Abstract

The unified defect model has been successful in explaining a wide variety of phenomena as oxygen or a metal is added to the 3-5 surface. These phenomena cover a range from a small fraction of a monolayer of adatoms to practical 3-5 structures with very thick overlayers. The tenets of the unified defect model are outlined, and the experimental results leading to its formulation are briefly reviewed. InP levels 0.4 and 0.1 eV and GaAs levels 0.7 and 0.9 eV below the conduction-band minimum (CBM) are associated with either missing column 3 or 5 elements. In InP, it has been found possible by a number of workers to "switch" between the two defect levels by variations in surface processing, temperature, and/or selection of the deposited atom. The need to apply the proper concepts for surface and interface chemistry and metallurgy is recognized, and the danger of using solely bulk concepts is emphasized. The reason for this is examined for certain cases on an atomic level. The need for new fundamental attacks on interface interactions is shown. The importance of semiconductor-oxide chemical stability is also recognized and, drawing on a large body of work from several laboratories, it is suggested that there will be more difficulties with "native" oxides on GaAs than on InP. It is

---

*Stanford Ascherman Professor of Engineering.

concluded that "scientific engineering" of interfaces to give optimum performance should be a goal and test of the fundamental work described here. Specific possibilities are discussed for Schottky barriers on 3-5's.

1. Introduction

At PCSI-6, the development of a unified model for Schottky-barrier and semiconductor-oxide interface states for 3-5 compounds was described (1). In that and subsequent papers (2,3), the experimental results were emphasized. Williams et al have reached similar conclusions for metals on inP (4). Additional evidence giving support to this model from a number of laboratories has appeared. We will not attempt a recompilation of all of this evidence here. Rather, appropriate reference will be given and, occasionally, comments will be made of specific results.

Emphasis will be placed on:

(1) The basic tenets underlying the unified defect model. It must be emphasized that these tenets resulted from a large body of experimental data.

(2) A brief review of the experimental evidence which led to or reinforced these tenets. This is followed by a section in which some additional evidence for the model is given.

(3) Up to this point, we have concentrated on first-order effects of the unified defect model; we follow this by a discussion of some detailed (second-order) points on which our knowledge is incomplete and/or in which better understanding of key phenomena is needed.

(4) The difficulties of simple extrapolations from bulk thermodynamics, to completely predict surface chemical and metallurgical phenomena. The need for "surface or interface thermodynamics and kinetics" will be discussed. By this we mean a "thermodynamics" characterizing the chemical interaction with the surface which takes place without completely breaking the chemical bonds between the surface atoms of semiconductor and the rest of the semiconductors; i.e. without the formation of bulk reaction products.

(5) Ways in which the defect model can be tested further, particularly by using it as a guide toward new methods of device fabrication which will optimize performance.

(6) The importance of the stability of "native oxides" at the interface and the role this plays in determining short- and long-term device life-time This year, additional attention has been focused on the stability of the native oxides of InP and GaAs, as reported in these proceedings and elsewhere. Thus, the implications of this new understanding both with regard to the unified defect model and in device applications will be discussed.

We have previously shown how the defect model was developed [5], and we will not repeat this here. However, it should be pointed out that Phillips' and Andrews' theoretical work [6,7] appear unique in anticipating the importance of metal-semiconductor metallurgical interaction in Schottky-barrier formation.

2. The Basic Tenets of the Unified Defect Model

For sake of clarity, we will outline the unified defect model in terms of certain tenets. However, it should be emphasized that these tenets were resulted from a large body of experimental data [7-11] and were formed to explain that data in the simplest most-straightforward manner possible.

Tenet 1: The surface of a 3-5 compound is strongly perturbed by placing less than a monolayer of oxygen or a metal on it.

Tenet 2: The surface perturbation results in the production of lattice defects at or near the interface.

Tenet 3: The defects produce the interface states which (1) characterize the 3-5-oxide interface or (2) produce Schottky-barrier pinning (see Fig. 1). Thus, a single mechanism determines the Schottky barrier height and position of 3-5: oxide interface states.

Figure 1 gives the energy levels, the acceptor or donor nature, and the missing element associated with each level [1,2]. These assignments will be examined in more detail later in this article. Suffice it to say here that these probably represent the simplest stable defects since the adatoms were applied [10,11] very "gently" and the samples were not heated. Thus, the energy levels in Fig. 1 (which are considered accurate to ±0.1 eV) represent the simplest defect levels stable at room temperature. The energy levels are most accurately known; the acceptor or donor nature of the defect is next-best known; whereas, there is the least certainty about the identity of the missing atom.

There are interesting systematics in the energy-level schemes of Fig. 1. Note the systematics of the levels in the band gaps of the three semiconductors. They fall in the top part of the band gap for InP and in the middle to lower region for GaAs. For GaSb, a single level is found near the valence-band maximum (VBM). It is likely that the second level lies below the VBM. It is worthwhile comparing these systematics with those found reported here by Daw and Smith [12].

3. A Brief Review of the Evidence which Led to the Unified Defect Model

Using photoemission spectroscopy to determine the surface Fermi-level ($E_{f,s}$) position [2,11], it was found for all three 3-5 compounds studied (GaAs, InP, and GaSb) that the $E_{f,s}$ is pinned, with less than ~1% of oxygen or 20% of a metal [1,2]. Figure 2 shows the surface E_f position versus Cs coverage and oxygen exposure for n- and p-type GaAs.

For a large range of elements with very different atomic orbits (see Fig. 3), e.g., Cs, In, Au, and oxygen, the pinning is independent of the element used [1,2,3]. This coincidence is independent of whether the pinning is near mid-gap or the conduction- or valence-band edges. In certain cases, for example, Cs, it is clear that the adatoms repell each other so that they must act essentially as atoms on the surface [13].

Based on the low coverage needed for pinning and independence of pinning energy on extreme changes in the chemistry of the adatom, it is concluded that the pinning mechanism must be indirect, i.e., that the pinning can not be due to levels directly introduced by the adatom, i.e., states that depend on the electronic orbitals of the adatoms. Rather, the new states must be generated indirectly, i.e., the perturbation of adatoms must create new energy states which do not depend on the electronic structure or other characteristics of the adatom [1,2,3].

Most importantly, there is a close correspondence in the pinning positions found in these experiments with submonolayer coverages of adatoms and those found in practical MOS or Schottky-barrier devices with many monolayers of adatoms [1,2,14]. This is critical since it establishes the connection between the basic studies leading to the defect model and practical devices. It also demonstrates that the essential mechanisms which determine the interface behavior in the 3-5's occur at

very low coverages.

Once the indirect nature of the formation of the new states becomes apparent, it becomes very attractive to assume that these new states are due to lattice defects induced by the adatom since this provides the simplest mechanism consistent with the large range available. For oxygen, both valence-band spectroscopy [8] and LEED [15] show that the surface becomes disordered at low coverage. It is easy to conceive how, in such a situation, vacancies or more complex lattice defects may be created. The fact that the clean surface is heavily strained [8,16,17] by the large surface rearrangement makes it easier to see how the surface may be disordered by a relatively small oxygen adsorption. For the thick oxides, evidence presented at PCSI-7 [18] and previously [16,19,20] indicates that the 3-5 atoms move through the oxide to the outer surface of the oxide before they react with the oxygen. This is in contrast to Si-SiO_2 where the oxygen moves through the oxide to react with the Si at the Si-oxide interface. The outward movement of the 3-5 atoms can aid in formation of additional defect states as the Ga and As atoms near the interface are consumed in the growth process. This is complicated by the nonuniform chemical spacial distribution in thick oxides.

The situation with regard to Schottky-barrier formation is also interesting. One of the most surprising results in the work leading to the unified defect model was the discovery that, even for metals where no appreciable chemical reaction was expected, the semiconductor material moves out into the deposited metal in surprisingly large quantities [1, 2,10]. This is now well documented in the literature [10], and a mechanism has been suggested [1,2,3] for it based on the heat of condensation

of the metal on the semiconductor.

There has been a mystery concerning Schottky barriers on 3-5's which the unified defect model clears up. On Si the Schottky-barrier height varies strongly, depending on the cleanliness of the surface on which it is deposited. In contrast 3-5 Schottky-barriers have been found to be surprisingly insensitive to the surface oxygen or oxidation. This is just what would be expected on the basis of the defect model (1,2,3) since the same defect levels and thus the same pinning position would be produced by oxygen or the metal; thus, the Schottky-barrier height on 3-5s would not be affected (to first order) by addition of oxygen to the surface before the metal.

It was these observations that led to the tenets listed in Part 2. Thus the tenets give as direct as possible a description of what is happening at the interface without recounting the detailed data which is outlined above and given in more detail elsewhere.

4. Switching between Interface States in InP

For at least two reasons, InP has turned out to be the 3-5 semiconductor material in which data from other sources has been most useful in testing the unified defect model. One reason is that the dominant energy levels which pin the Fermi level appear to be relatively easily switched between the two levels shown in Fig. 1. This is probably partially due to the fact that the donor level lies above the acceptor level-producing compensation so that the pinning level for either n- or p-type InP may be switched by a relatively small change in the relative density of defects. It is also clear from a large range of work (10,21,22,23) that the surface oxide is more stable on InP than GaAs or GaSb. This may

allow for a lower and better-controlled density of defect levels. We will return to the discussion of the surface oxides later.

In Fig. 4, we indicate the density of interface states present on MOS structures formed by different detailed processing by Wieder and his coworkers and by Fritsche [24]. Note that, in the first case, the density of interface states peaks sharply at about 0.1 eV and, in the latter, at about 0.4 eV below the CBM. At first glance, these results (which were reported after the unified defect model was proposed(1)) might seem confusing. However, if one notes that the two levels coincide with the two defect levels in Fig. 1, the explanation becomes straightforward. In the case of the 0.1 eV result, the processing must ensure that this level dominates; whereas, the reverse is true for the 0.4 eV result. In fact, Wieder and his coworkers [25] have been able to obtain the 0.4 eV result by slight variations in preparation of the very thin natural (~10 Å) oxide before capping the natural oxide with a thick protective layer of SiO_2 or a similar insulator. Thus the data of Fig. 4 can be understood by the unified defect model and also show how sensitive the surface can be to slight changes in chemical processing.

Since we will next turn to the attempt to identify the nature of the defect levels at about 0.1 and 0.4 eV in InP, it should be mentioned that Wilmsen and Wagner [26] found excess indium in the oxide of the MOS structure formed in a similar manner to those of Wieder and coworkers, which were dominated by the 0.1 eV level. The simplest explanation of this would be that this method of preparation produces an In deficit and thus associates a defect produced by missing In with the 0.1 eV level.

5. Other Examples of Shifting between the 0.1 and 0.4 eV Levels in InP and Difficulties in Definitively Determining the Defect Responsible for those Levels

In Fig. 1, we have associated the 0.1 and 0.4 eV levels with defects associated with missing In and P atoms, respectively; however, in discussing Fig. 1, we indicate the uncertainty in that assignment. In fact, Williams [4] and his coworkers have also concluded that the defect model is applicable but have suggested that the 0.1 eV acceptor is due to a missing P and the 0.4 eV level to a missing In, assignments opposite to those of Fig. 1. In this section, we want to do three things: (1) help establish the overall validity of the model by showing how details of surface processing can shift the level dominating the Schottky-barrier pinning position between the 0.1 and 0.4 eV levels, (2) through these shifts and the details of their production, emphasize the importance of surface and interface chemistry in determining the dominant interface state, and (3) show that there is contradictory data as to whether the 0.1 and 0.4 eV levels are, respectively, due to missing In or P. Implicit in the third item is the recognition that we do not yet fully understand the surface and interface interactions which determine the nature of the defects. The problems inherent here are related to some of the considerations of Brillson [27], with the exception that he did not consider the defect mechanism suggested here and he appeared to attempt to explain Schottky-barrier pinning solely in terms of bulk thermodynamics.

Previously, we pointed out the evidence of Wilmsen and Wagner [26] for the 0.1 eV level being due to a missing Ga. The work of Farrow et al also offers evidence for this [28]. An Ag overlayer usually provides a Schottky-barrier height near 0.4 eV on n-type InP. (Since we have limited the accuracy of the assignments made in Fig. 1 to about $\pm$ 0.1 eV,

the reader should not be concerned that this level is found at 0.5 eV by Williams et al [4].) However, when the InP surface in a MBE (molecular beam epitaxy) apparatus was terminated with P before the Ag was added, $E_{f,s}$ is pinned at 0.1 eV. This suggests that the 0.4 eV level is due to a P deficit since one would expect the P termination to supress the P defect formation and allow defects due to missing In to dominate. Thus, the data supported identifying the 0.4 eV level with missing P.

However, Williams et al [4] report that oxygen, chlorine, and other gases can cause a depletion of P near the surfaces (this depletion is assigned to formation of a volatile species which leaves the surface). When Au, Cu, or Ag, which normally produce the 0.4 eV Schottky barrier, are evaporated onto this surface, the 0.1 eV Schottky barrier is found. Thus, evidence is given that the 0.1 eV level is due to missing P. Williams et al [4] also find that Ni and Fe, which form exothermic compounds with P, produce the 0.1 eV Schottky-barrier pinning; whereas, Au, Ag, and Cu, which do not, form a 0.4 eV Schottky barrier on clean InP. If the Ag or Au Schottky barriers are annealed at 300°C [29], the barrier height reduces to the 0.1 eV level and evidence is found for In diffusion into the Ag (as well as Ag diffusion into the InP). The shift to the 0.1 eV pinning level accompanied by the diffusion of In from the InP is taken as evidence for the formation of defects due to missing In and, thus, support that view of identification of the 0.4 eV level.

Williams et al also find that In forms a 0.1 eV Schottky barrier, thus, supporting the proposition that the 0.1 eV is due to missing P. Theoretical work by Srivastava [30] indicates that P forms a donor level near 0.1 eV. However, although rapid progress is being made on the theory of vacancies [1,2,31] in the III-V and while the theoretical results seem to agree

well with the general trends, it would be premature to say that complete theoretical understanding has been obtained (see Ref. 12).

In Fig. 5, we present data of the surface Fermi-level position for n- and p-type InP as a function of oxygen exposure found by Chye et al [10]. We direct the reader's attention to the fact that, on n-type InP, $E_{f,s}$ drops to about 0.4 eV below the CBM before rising and stabilizing at about 0.1 eV below the CBM. Street et al [32] have found that, using this behavior, they obtain a straightforward explanation of their photoluminescence data. Note also that the surface E_f in the p-type material appears to rise above 0.4 eV for the highest exposures in Fig. 5.

The importance of the "reversal" shown in Fig. 5 is that it indicates that the 0.1 and 0.4 eV levels must be donors and acceptors, respectively, since this reversal can only be understood in terms of such a compensating pair of levels. At the lower oxygen exposures, a dominant density of the 0.4 eV level must be produced; whereas, with increasing oxygen uptake, the 0.1 eV level (a donor) must become dominant since it pins the Fermi level. This reversal of the dominant defect level illustrates the subtleties of the surface chemistry going on. Likewise, a rise of $E_{f,s}$ for the p-type material above 0.4 eV suggests that the 0.1 eV level is a donor.

Thus, we conclude that there is good agreement on the energy as well as on donor vs acceptor identification of the defect producing the level. However, the identity of these defects (even knowledge of which deficiency - column 3 or 5 - the defect is due to) remains to be definitively determined.

6. Difficulty of Using Bulk Thermodynamics in Dealing with Surface Chemistry and the Need for "Surface" Thermodynamics and Kinetics

In opening PCSI-7, Prof. Gatos (33) has emphasized the fundamental need for a better understanding of the reactions of ambients with surfaces. Here, we reemphasize that need and focus on certain aspects of the problem.

An example of a departure from bulk thermodynamics is our suggestion that it is the heat of condensation of the metal on the 3-5 materials which is responsible for the appearance of semiconductor mater in the metal during deposition [1-3,5]. This heat of condensation has been studie definitively only for Cs on GaAs (34) where the heat of condensation on a clean GaAs surface is three times larger (approximately 60 Kcal/mole) than for Cs on Cs (approximately 20 Kcal/mole). The large heat of condensation for Cs on GaAs is associated with the very strong polarization of the Cs atom by the free surface--a phenomena first studied and explained by Langmuir for Cs on metals many decades ago. Such polarization effects a undoubtedly important for Al, In, and other metallic atoms placed on 3-5's or other semiconductors; however, these effects probably decrease with increasing ionization energy of the outmost electron(s) in the adsorbed atom. Elsewhere in this volume [35], certain aspects of the bonding of Al and Ga to GaAs are discussed. There is general evidence that the heat of condensation of metals on semiconductors is large [1,2]; however, there is need for much more precise studies of this.

Abbati et al [36] have shown by temperature studies that the heat of condensation of Au on Si is important in the intermixing which takes place between the semiconductor and the metal. In addition, they show that ambient thermal agitation also plays a role. Braicovich et al [37] have also reported that, for Si, the formation of silicides, even weakly bound silicides, is important. Only in the case of Ag where no silicide is formed has no intermixing been found for Si. Intermixing has been found for all 3-5:metal systems (including Ag) tried to date. The difference Williams et al [4] found between the noble metals and the transition metals on InP indicates that relative

number of columns 5 and 3 defects may depend on bulk chemistry. Thus, it is clear that in some cases such as Cs on semiconductors, bulk chemistry plays a negligible role. However, in other cases, both surface energies (e.g., the heat of condensation) and the bulk chemistry are important. It can not be overemphasized that much more effort should be placed in understanding these phenomena since interface chemistry is not only of such critical importance to the semiconductor and other industries but is essential if fundamental insight is to be gained.

Before closing this section, it is important to refer the reader back to Fig. 2 and remind him that the surface Fermi-level pinning is usually completed by the time less than 20% of a monolayer has been applied for the metals and semiconductors shown in Fig. 3. Williams et al [4] also report this to be the case for Ag on InP. It would be important, for example, to study $E_{f,s}$ versus coverage as a function of temperature as has been done for Si [36] for materials such as Fe and Ni on InP where bulk reactions appear to play an important role in determining the relative density of defect levels due to missing In or missing P in InP. In this way, the relative importance of the heat of condensation, bulk reactions, and thermally stimulated processes might be determined.

It appears from the work of Williams et al [4] that Al on InP is another interesting system. At 77° K, the 0.4 level appears to dominate; whereas, at room temperature, it is the 0.1 eV level which dominates.

7. The Possibility of "Scientifically Engineering" Schottky-Barrier Heights

In this section, we will attemp to give an example of how the knowledge we now have of interfaces may lead to new "scientific engineering" of our circuit component.

Once it is realized that Schottky-barrier heights are determined by extrinsic states, i.e., the defect states formed by depositing the metal, one can start envisioning ways in which Schottky-barrier heights can be "scientifically engineered" to give optimum performance for a given

application (3). In the previous section, it has been indicated that the relative density of defect levels may be increased or decreased by various techniques. For example, by terminating the lattice with P, the desnity of defect levels due to missing P may be reduced, or, by making the Schottky barrier on InP with In and perhaps annealing, the density of In defects may be reduced.

Although these approaches can reduce the number of defects, a new element must be introduced in order to obtain more complete control of the barrier height. This is extrinsic doping of the surface with an impurity giving the desired barrier height. By reducing the defect state density, it may be possible to make the surface impurity doping dominate. For example, if a maximum barrier height was desired on n-type GaAs (or InP), the GaAs surface could be terminated with As (P), the Schottky barrier formed using Ga (In) (probably in an alloy with higher melting temperature than pure Ga (In)) with, perhaps, some annealing to make it available to minimize the defects due to missing Ga and As (In and P). However, before this final processing, the last 10 or 20 layers of GaAs (InP) could be grown to contain a large density of an acceptor such as Zn or Be so that the Zn acceptor levels could dominate the defect levels and pin $E_{f,s}$. This could be done, for example, by MBE. Similar procedures can be thought of for other 3-5's and/or other barrier heights. This may not be an easy process to develop since there may be interactions between the variables as is suggested by the conflicting results given in Section 5 and in the discussions of Section 6. However, the

importance of being able to control Schottky-barrier heights make this an intriguing path to follow. In doing so, it is also likely that we will learn more about the questions raised in the last section concerning the interrelations between bulk and surface chemistry and also to provide further testing and refinement of the unified defect model.

8. The Stability of "Native Oxides" on GaAs, InP, and GaSb

It would be misleading not to make contact between the preceding discussions and recent advances in understanding of the stability of the "native oxides" of GaAs and InP. In order to make contact between our own work and that reported at PCSI-7 or elsewhere, we will first review some of our own prior results. Using ultrahigh vacuum apparatus and synchrotron radiation, earlier work had indicated that stability of the 3-5 compounds studied under various exposures to oxygen decreased in the order of InP, GaAs, and GaSb. To illustrate this, we present in Fig. 6 spectra of the core states of InP and GaAs in the atomically clean (vacuum cleaved) state after a heavy exposure to unexcited oxygen (i.e., oxygen in the molecular ground state) and, lastly, after exposure to excited oxygen (i.e., to oxygen which contained either the excited molecular in a metastable state and/or atomic oxygen) [8,10,23].

The peaks in Fig. 6 give the binding energy of the highest-lying core state of the two components in each semiconductor. For the clean curves, there are only two core peaks--one for each element in the compound. As chemical bonding take place, new peaks appear.

The area under the set of peaks associated with one element is portional to the amount of that element within a depth given by the electron escape depth (about 5 Å) of the surface.

As can be seen from Fig. 6, InP forms a stable compound on exposure to unexcited oxygen. (Our criteria for its being stable is that it is not affected by exposure to excited oxygen.) In contrast, exposure to excited oxygen plays havoc with the GaAs. In that material, a number of new As peaks appear and there is a net loss of As from the surface. One of the peaks has been identified as elementary As. Thus, it is clear that InP forms a more stable surface oxide than GaAs.

Much more definitive work has been recently done on the phase diagram and stability of GaAs and InP. The reader is referred to reports on this made at PCSI-7 by, for example, Schwartz et al [21] and Lucovsky and Bauer [22]. A number of other papers reflect the kinetics as well as thermodynamics of the formation of "native oxide" under different conditions [38-46]. The work of Schwartz et al, Lucovsky, and ourselves *all point to greater thermodynamical stability for* InP than GaAs native oxides in the presence of InP or GaAs. Of extreme importance is the determining of the Ga-As-O phase diagram by Schwartz et al and their conclusion from this that As oxide is not thermodynamically stable in the presence of GaAs. The phase diagram indicates, for example, that the following reaction will take place.

$$2GaAs + As_2O_3 \rightarrow Ga_2O_3 + 4As$$

This is probably why we see elementary As in Fig. 6. More importantly, it means that, at the GaAs oxide interface, GaAs is not thermodynamically stable in the presence of As oxides. However, what is not yet known is the thermal activation barrier against this reaction. Device experience suggests stability at room temperature and low electric fields. A key question is at what temperature (and electric fields) will the activation

barrier be overcome and the reaction take place, i.e., is the stability of GaAs "native oxides" sufficient to allow for easy device fabrication and long-term operation. This is still an open question; however, the history of device fabrication and/or life with these materials can give us some clues.

GaAs FETs, LEDs, and lasers (the latter two utilizing GaAlAs as well as GaAs) have been fabricated and successfully put into practical use. On the other hand, no real success has been had to date with GaAs MOS structures despite a very large effort. This is partially due to the depth of the defect levels as shown by Fig. 1; however, the density of defect levels may be increased significantly larger in GaAs due to the oxide instability.

For a variety of reasons, including the scarcity of material, there is much less experience with InP than GaAs. As a rough estimate, one might say that perhaps 1% of the effort has been put into InP MOS, LED, and laser activities as in the same activities using GaAs. (The "GaAs" LED's are formed from GaAlAs and GaAs on a GaAs substrate; whereas, the "InP" LED's and lasers are InGaAsP grown on InP.) Realizing the difference in the amount of effort to date, the result for the two materials are striking. "InP" LED's appeared to have much greater time stability (i.e. much longer life) particularly at higher currents and/or temperatures. It appears that "device quality" InP MOS structures have been built (24)

Wieder [24] has described in this volume work with InP MOS structures and suggests a mode of operation for IC-type applications. We would like to emphasize several aspects of this work. First, the successful InP MOS devices are formed by forming only a very thin (~10 Å) native oxide layer

and then depositing a thick layer of SiO_2 or another insulator. A similar procedure has been proven effective for InSb by Langen [47]. We had earlier suggested, based on studies such as those illustrated in Fig. 6, that such procedures could be profitable [23]. This was based on the observation that, even for GaAs, thin oxides formed in our ultrahigh vacuum experiments should be more stable than thicker oxides. Most importantly, the variety of As compounds, elementary As, and As loss occurred only with the thicker oxides: It was necessary to use excited oxygen to form these.

Another factor probably arises in the case of InSb where the minimum thickness native oxide followed by a thick deposited oxide procedure has been successfully applied by Langen [47]. In addition to the advantages of surface preparation procedure, another factor may be important in InSb. The simple defect states, such as those shown in Fig. 1, may lie outside the band gap of InSb. Note, in Fig. 1, that, for GaSb with a band gap of only 0.6 eV, a single state lies in the band gap, not two as in the case of the wider band-gap materials. The state in the gap is an acceptor long associated with a missing Sb; thus, the other state must be a donor and it most probably lies below the VBM, i.e., it is degenerate with the valence band. Theoretical calculations also raise the possibility of defect levels lying in the valence and/or conduction band [12].

To summarize this section up to this point, we have pointed out the difference in the relative stability of oxides of two of the 3-5's. This difference appears to be important in determining the density of interface states. It may also be important in determining the long-term stability of 3-5 oxide interfaces. GaAs has a tendency toward instability in presence of As oxides; however, this does not seem to be the case for InP and P_2O_5. This instability of As oxides may lead to a long term problem with leakage at the oxide-GaAs interfaces. Such interfaces are necessary even for FETs. Whether there is any connection between the increased life of InP-based LEDs (particularly at elevated temperatures) as compared to GaAs LEDs and the oxide stability is yet to be definitively established; however, the presently available information is suggestive.

Thus, in choosing materials for devices, not only must one be aware of the defect levels but one must also understand much better the long-term stability of the interface oxides. A similar situation arises in the Schottky barriers, contacts, or other metallization [48-53]. One must be aware of the defects (see Fig. 1) inherent in formation of contacts, but one must also try to understand the chemical and metallurgical interactions between the metals and semiconductor components at the interface since these determine the details of the relative densities of the states involved as well as other important properties, such as long term stability. Above all, it is important to start exploring ways to reduce the defect density at Schottky-barrier interfaces and using surface or interface doping to obtain optimum Schottky-barrier heights for a given application.

9. Conclusions

The unified-defect model appears to explain a wide variety of data extending from 3-5 surfaces with adatoms to 3-5's with thick overlayers. There is an extreme need to better understand the chemical interactions at interfaces on an atomic scale and to work out the thermodynamics and kinetics involved with interface formation. Not only is this an important frontier of fundamental science, but it has extremely important implications as the size of integrated systems is reduced and their speed increased. If fundamental understanding is not gained rapidly, great waste can result.

Acknowledgment

One of the authors (WES) has profited strongly from discussions with W. Goddard, T. McGill, J. C. Phillips, and A. Zunger.

This work was supported by the Advanced Research Projects Agency of the Department of Defense and was monitored by the Office of Naval Research under Contract No. N00014-79-C-0072 and by the Office of Naval Research, N00014-75-C-0289. Part of the work was performed at SSRL which is supported by the National Science Foundation, NSF DMR 77-27489, in cooperation with the Stanford Linear Accelerator Center and the Department of Energy.

References

1. W. E. Spicer, P. W. Chye, P. R. Skeath, C. Y. Su, and I. Lindau, J. Vac. Sci. and Tech. 16, 1422 (1979) and references therein.

2. W. E. Spicer, P. W. Chye, P. R. Skeath, and I. Lindau, Inst. of Phys. Conf. Ser. No. 50, p. 216, Bristol (1979).

3. W. E. Spicer, I. Lindau, P. R. Skeath, C. Y. Su, and P. W. Chye, Phys. Rev. Lett. 44, 420 (1980).

4. R. H. Williams, R. R. Varma, and V. Montgomery, J. Vac. Sci. and Tech. 16, 1418 (1979); T. Humphreys, M. H. Patterson, and R. H. Williams, these proceedings and references therein.

5. I. Lindau, P. W. Chye, C. M. Garner, P. Pianetta, C. Y. Su, and W. E. Spicer, J. Vac. Sci. and Tech. 15, 1332 (1978).

6. J. C. Phillips, J. Vac. Sci. and Tech. 11, 947 (1974).

7. J. M. Andrews and J. C. Phillips, Phys. Rev. Lett. 35, 56 (1975).

8. P. Pianetta, I. Lindau, P. E. Gregory, C. M. Garner, and W. E. Spicer, Surf. Sci. 12, 298 (1978) and references therein; I. Lindau, P. Pianetta, C. M. Garner, P. W. Chye, P. E. Gregory, and W. E. Spicer, Surf. Sci. 63, 45 (1977).

9. P. E. Gregory and W. E. Spicer, Phys. Rev. B12, 2370 (1975); Phys. Rev. B13, 725 (1976); Surf. Sci. 54, 229 (1976) and references therein.

10. P. W. Chye, I. A. Babalola, T. Sukegawa, and W. E. Spicer, Phys. Rev. Lett. 35, 1602 (1975); Phys. Rev. B13, 4439 (1976); P. W. Chye, C. Y. Su, I. Lindau, C. M. Garner, P. Pianetta, and W. E. Spicer,

Surf. Sci. 88, 439 (1979); P. W. Chye, I. Lindau, P. Pianetta, C. M. Garner, C. Y. Su, and W. E. Spicer, Phys. Rev. Lett. B18, 5545 (1978); C. Y. Su and P. Skeath, to be published.

11. P. Skeath, I. Lindau, P. W. Chye, C. Y. Su, and W. E. Spicer, J. Vac. Sci. and Tech. 16, 1143 (1979) and references therein.

12. M. S. Daw and D. L. Smith, these proceedings and references therein.

13. J. Derrien and F. A. D'Avitoya, Surf. Sci. 65, 688 (1977) and references therein.

14. W. E. Spicer, I. Lindau, P. Pianetta, P. W. Chye, and C. M. Garner, Thin Solid Films 56, 1 (1979); W. E. Spicer, P. W. Chye, C. M. Garner, I. Lindau, and P. Pianetta, Surf. Sci. 86, 763 (1979).

15. A. Kahn, D. Kanani, P. Mark, P. W. Chye, C. Y. Su, I. Lindau, and W. E. Spicer, Surf. Sci. 87, 325 (1979).

16. W. E. Spicer, P. Pianetta, I. Lindau, and P. W. Chye, J. Vac. Sci. and Tech. 14, 885 (1977).

17. W. E. Spicer, I. Lindau, J. N. Miller, D. T. Ling, P. Pianetta, P. W. Chye, and C. M. Garner, Physica Scripta 16, 388 (1977); D. J. Chadi, Phys. Rev. Lett. 41, 1962 (1978) and references therein.

18. C. W. Wilmsen, R. W. Kee, and K. M. Glib, J. Vac. Sci. and Tech. 16, 1434 (1979) and references therein.

19. C. C. Chang, B. Schwartz, and S. P. Muraku, J. Elec. Chem. Soc. 124, 922 (1977).

20. K. H. Zaininger and A. G. Revesy, J. Phys. (Paris) 25, 208 (1976).

21. G. P. Schwartz, C. D. Thurmond, G. W. Kammlott, and B. Schwartz, these proceedings; G. P. Schwartz, G. J. Guntheri, G. W. Kammlott, and B. Schwartz, J. of Elec. Soc. and references therein, in press.

22. G. Lucovsky and R. S. Bauer, these proceedings.

23. W. E. Spicer, P. Pianetta, I. Lindau, and P. W. Chye, J. Vac. Sci. Tech. 14, 885 (1977).

24. H. H. Wieder, Inst. of Phys. Conf. Ser. No. 50, Bristol (1979); H. H. Wieder, these proceedings and references therein.

P. Fritzche, Inst. of Phys. Conf. Ser. No. 50, Bristol (1980).

25. H. H. Wieder, private communication.

26. C. W. Wilmsen and J. R. Wagner, Inst. of Phys. Conf. Ser. No. 50, Bristol (1979).

27. L. J. Brillson, Phys. Rev. Lett. 40, 28 (1978); L. J. Brillson, R. Z. Bachrach, R. S. Bauer, and J. McMenamin, Phys. Rev. Lett. 42, 397 (1979).

28. R. E. C. Farrow, A. G. Cullis, A. J. Grant, and J. E. Patterson, J. of Cryst. Growth 45, 292 (1978). R.E.C.Farrow, A.G.Cullis, A.J.Grant, G.R.Jones, and R.Clampitt, Thin Solid Films 58, 189 (1979)

29. R. H. Williams, R. R. Varma, and A. McKinley, J. Phys. C. 10, 4545 (1979).

30. G. P. Srivastava, to be published.

31. H. P. Hjalmarson, R. E. Allen, H. Buttner, and J. D. Dow, these proceedings.

32. A. A. Street, R. H. Williams, and R. S. Bauer, these proceedings.

33. H. C. Gatos, these proceedings.

34. J. Derrien and F. A. D'Avitoya, Surf. Sci. 65, 668 (1977).

35. P. R. Skeath, C. Y. Su, I. Lindau, and W. E. Spicer, these proceedings and references therein.

36. I. Abbati, L. Braicovich, A. Franciosi, I. Lindau, P. R. Skeath, C. Y. Su, and W. E. Spicer, these proceedings.

37. L. Braicovich, I. Abbati, G. Ottaviani, J. N. Miller, S. Schwartz, P. R. Skeath, C. Y. Su, C. R. Helms, I. Lindau, and W. E. Spicer, these proceedings.

38. K. M. Glib and C. W. Wilmsen, these proceedings.

39. K. Yamasaki and T. Sugano, these proceedings.

40. C. Y. Su, I. Lindau, P. W. Chye, P. Skeath, and W. E. Spicer, these proceedings.

41. W. Monch and R. Enninghorst, these proceedings.

42. D. W. Langer, F. L. Schuermeyer, J. Johnson, M. L. Hartnogel, H. P. Singh, and C. W. Litton, these proceedings.

43. D. A. Boglee, D. K. Ferry, C. W. Wilmsen, and H. H. Wieder, these proceedings.

44. P. J. Gunthaner, R. P. Vasquez, and F. L. Gunthaner, these proceedings.

45. L. L. Kamerski, P. J. Ireland, P. Sheldon, T. L. Chu, S. S. Chu, and C. L. Lin, these proceedings.

46. A. Ebina, K. Asano, Y. Suda, and T. Takahashi, these proceedings.

47. J. D. Langen, private communication.

48. L. J. Brillson, G. Margaritondo, N. G. Stoffel, R. S. Bauer, B. Z. Bachrach, and G. Hansson, these proceedings.

49. D. V. Morgan, C. J. Palmstrom, and J. Smith, these proceedings.

50. T. F. Kuech and J. O. McCaldin, these proceedings.

51. R. W. Bene, R. M. Walser, G. S. Lee, and K. C. Chen, these proceedings.

52. W. Gopel, L. J. Brillson, C. F. Bucker, and R. S. Bauer, these proceedings.

53. M. J. Cohen, M. D. Paul, D. L. Miller, and J. S. Harris, Jr., these proceedings.

Figure Captions

1. The defect energy levels induced by overlayers on GaAs, InP, and GaSb. In panel (a), the position in energy donor or acceptor nature of the defect is shown as well as a suggestion as to the missing atom responsible for the defect. Panel (b) indicates the defects against the continuum of interface states usually found at semiconductor-oxide interfaces. Si is included for comparison. The results shown indicate no peak in the $Si:SiO_2$ interface state density, as is normally found experimentally; however, N. M. Johnson, D. J. Bartelink, and J. P. McVittie [J. Vac. Sci. Technol. 16, 1407 (1979)] have found that, if hydrogen is not present, there is a peak of "dangling bond" states about 0.3 eV above the VBM.

2. The surface Fermi-level pinning position ($E_{f,s}$) for p- and n-type GaAs as it is changed by adatoms. Panel (a) shows E_f versus coverage for various metals. Panel (b) gives E_f versus coverage as oxygen is added. Unexcited oxygen was used for the n-type GaAs [8]. The solid line for p-type was taken using excited oxygen [9]; the points are for unexcited oxygen [10].

3. The final pinning position for various adatoms on GaAs, InP, and GaSb. The coverage is given in units of $10^{15}/cm^2$ [the GaAs (110) surface has $9 \cdot 10^{14}$ atoms/cm^2).

4. The interface state density for MOS produced by different preparation techniques. That of Wieder and coworkers is dominated by the 0.1 eV level (see Fig. 1); that of Fritsche by the 0.4 eV level.(24)

5. $E_{f,s}$ versus oxygen exposure for InP. Note how $E_{f,s}$ for the n-type sample drops and then rises. This suggests that, at very low coverages, the acceptor defect at 1.2 eV dominates; whereas, at high coverages, the donor defect becomes dominant.

6. The different effects of unexcited and excited oxygen on GaAs (panel a) and InP (panel b). These results [10] show the greater stability of native oxides of InP than of GaAs, a conclusion supported by other work [21,22]. The top curve in each panel is the clean or cleaved semiconductor. The second curve shows the effect of exposure to the indicated dose of unexcited oxygen. In the bottom two curves, the effect of oxygen excited, E.O., by the ion gauge is shown. The position of the ion gauge with respect to sample was the same in all cases. The heavily oxidized and very heavily oxidized spectra for the GaAs surface were obtained by added $5 \cdot 10^5$ L of E.O. to the previous exposure and with ion gauge currents of 0.4 and 4 mA, respectively.

UNIFIED MODEL FOR INTERFACE
STATES AND SCHOTTKY BARRIERS

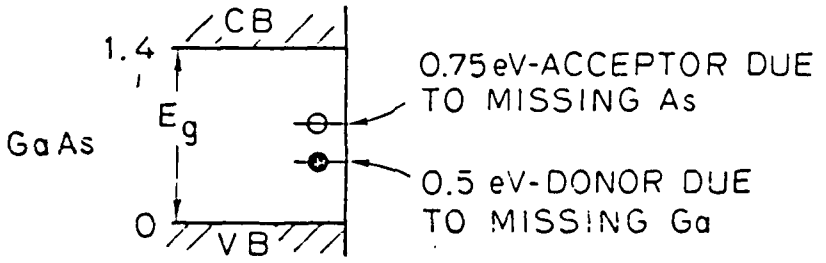

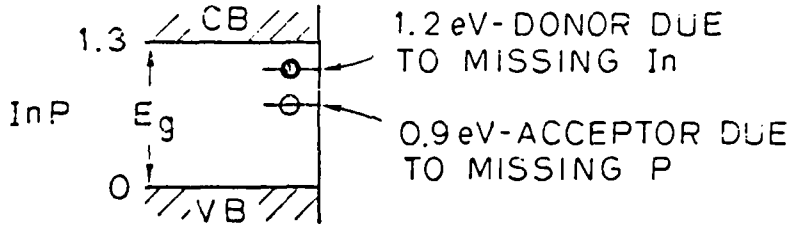

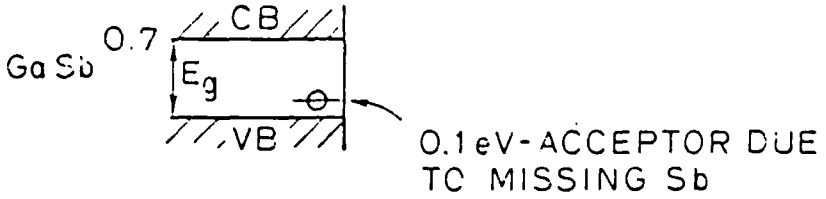

Fig. 1a

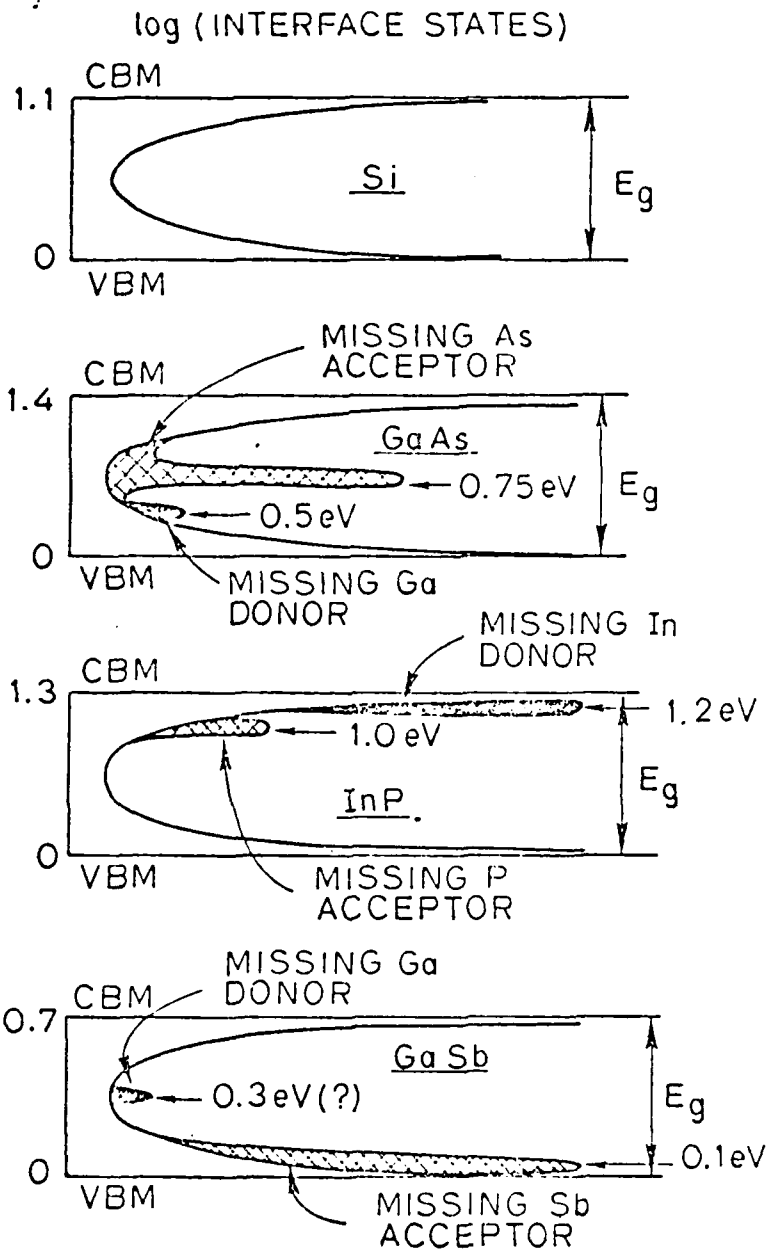

INTERFACE STATE: SEMICONDUCTOR OXIDE

Fig. 12

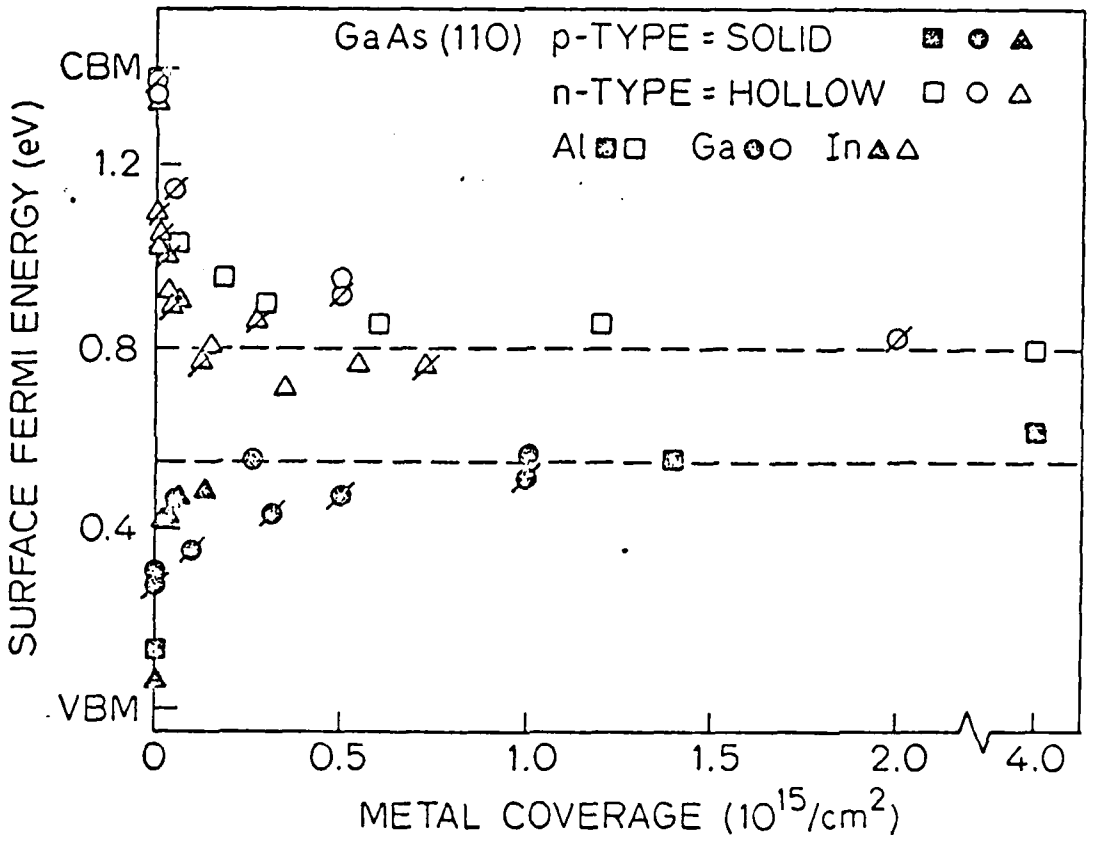
GaAs (110) p-TYPE = SOLID
n-TYPE = HOLLOW
Al Ga In
CBM
1.2
0.8
0.4
VBM
SURFACE FERMI ENERGY (eV)
0
0.5
1.0
1.5
2.0
4.0
METAL COVERAGE (10^{15}/cm^2)

Fig. 29

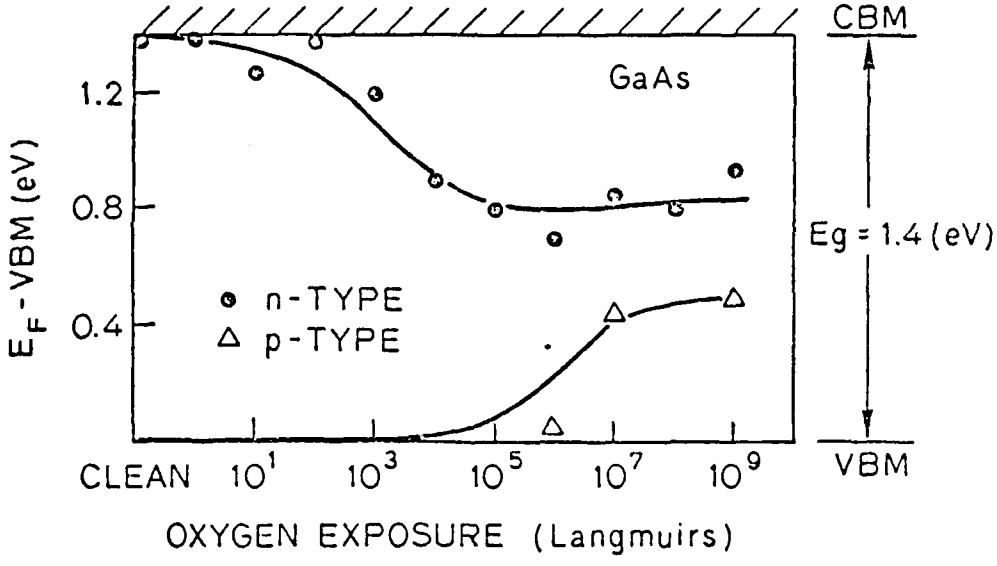
CBM
GaAs
1.2
0.8
0.4
E_F - VBM (eV)
n-TYPE
p-TYPE
Eg = 1.4 (eV)
CLEAN
10^1
10^3
10^5
10^7
10^9
VBM
OXYGEN EXPOSURE (Langmuirs)

Fig. 2a

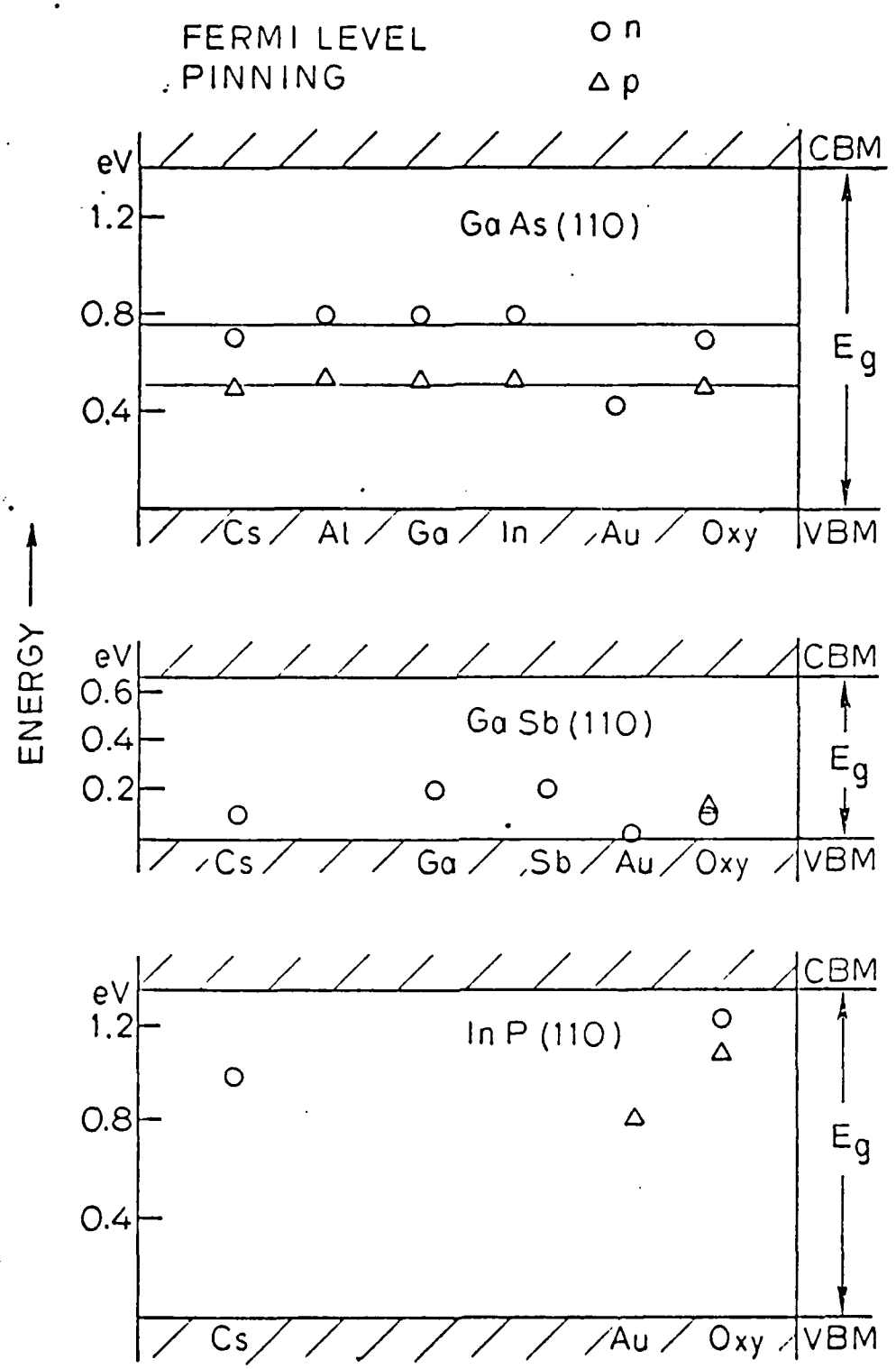

OVERLAYER PRODUCING PINNING (Sub-Monolayer)

Fig. 3

MOS DEVICES

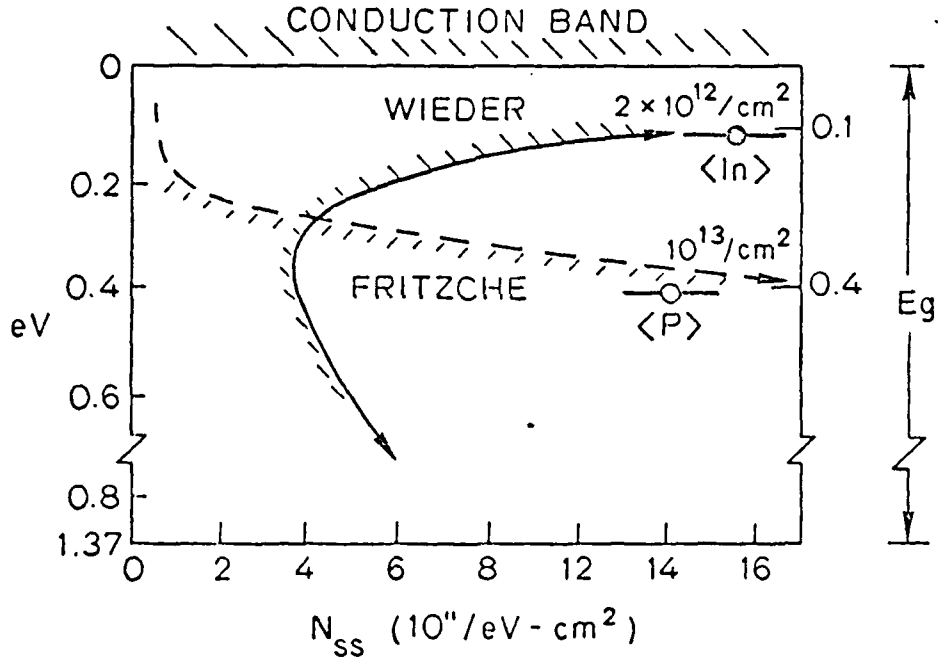

Fig. 4

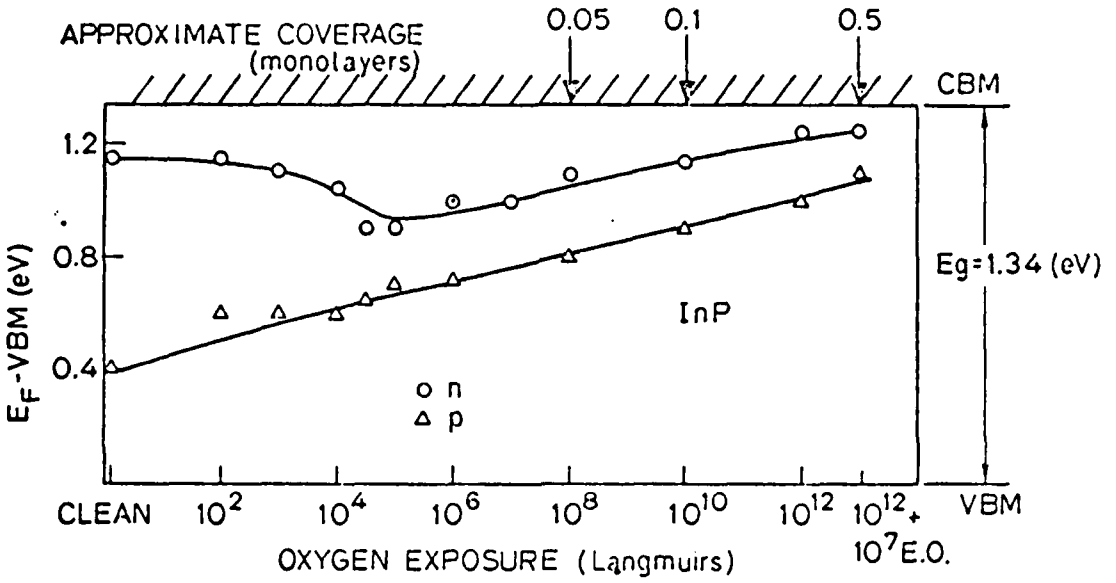
APPROXIMATE COVERAGE
(monolayers)
0.05
0.1
0.5
CBM
1.2
0.8
0.4
E_F-VBM (eV)
Eg=1.34 (eV)
InP
o n
Δ p
CLEAN
10^2
10^4
10^6
10^8
10^{10}
10^{12}
10^{12}+
10^7E.O.
VBM
OXYGEN EXPOSURE (Langmuirs)

Fig. 5

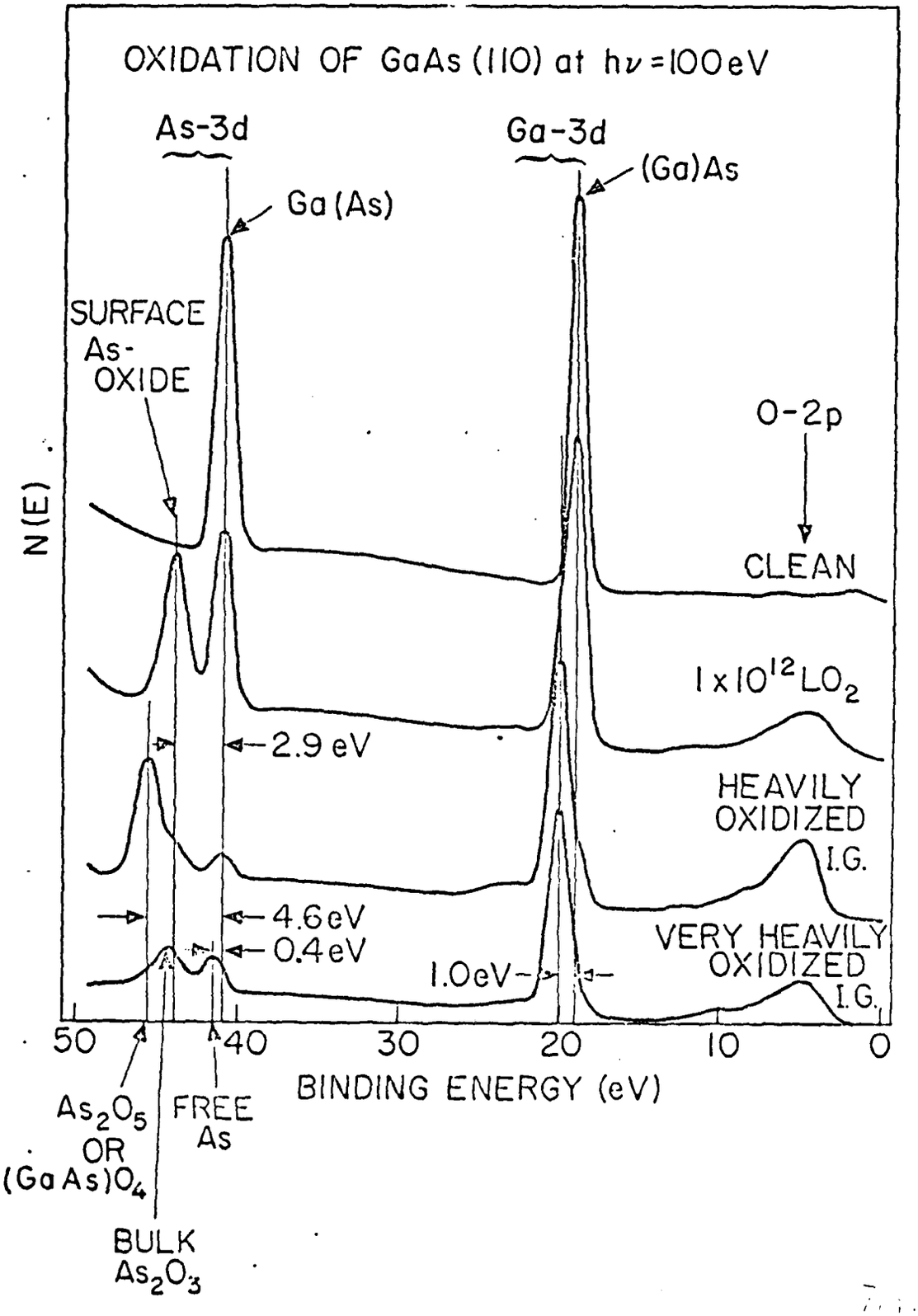
OXIDATION OF GaAs (110) at hν = 100 eV
As-3d
Ga-3d
Ga (As)
(Ga) As
SURFACE As-OXIDE
O-2p
CLEAN
1 x 10^12 LO2
2.9 eV
HEAVILY OXIDIZED
I.G.
4.6 eV
0.4 eV
1.0 eV
VERY HEAVILY OXIDIZED
I.G.
N(E)
50
40
30
20
10
0
BINDING ENERGY (eV)
As2O5 OR (GaAs)O4
FREE As
BULK As2O3

Fig. 6-4

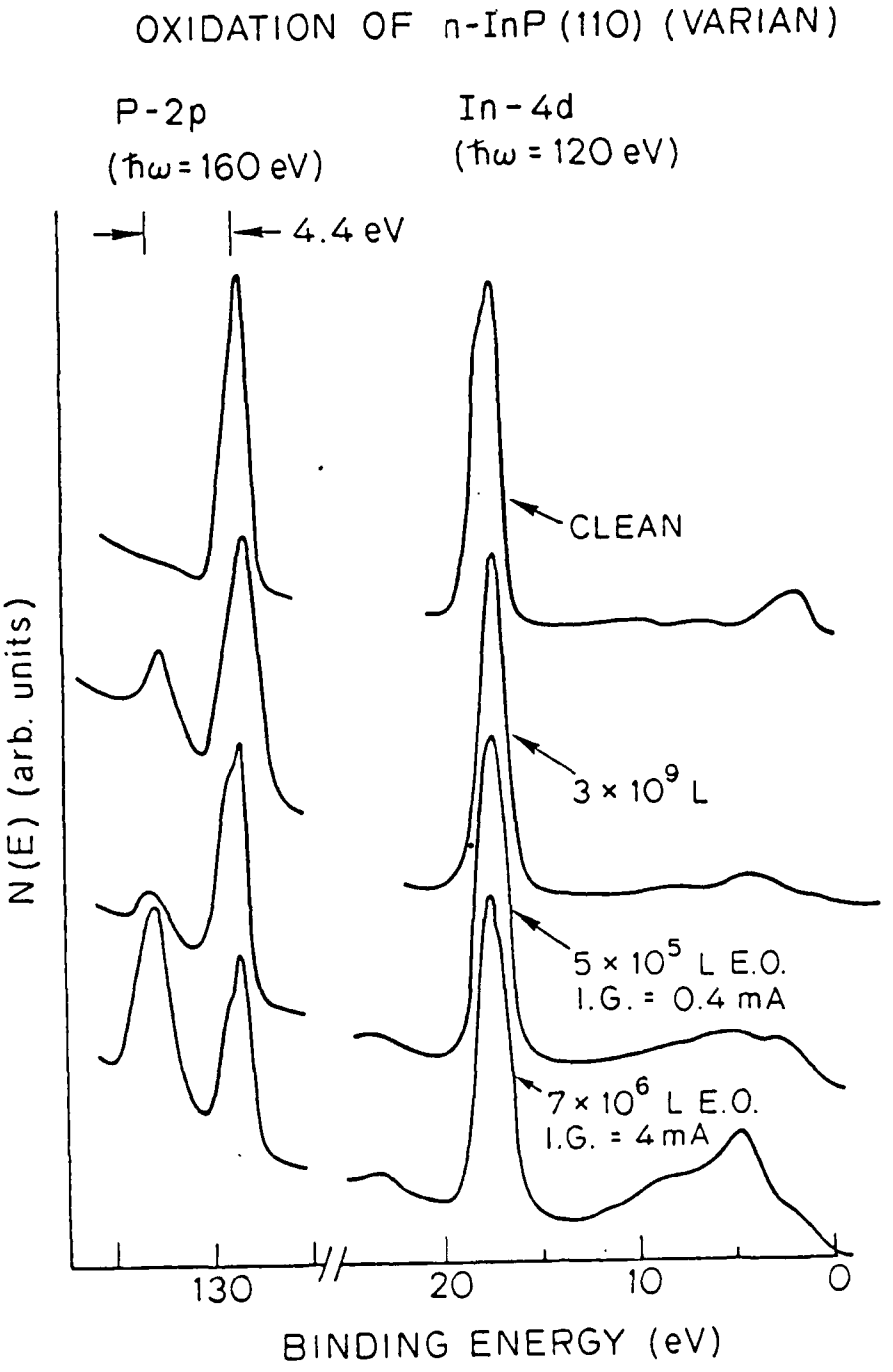
OXIDATION OF n-InP (110) (VARIAN)
P-2p
(ħω = 160 eV)
In-4d
(ħω = 120 eV)
4.4 eV
CLEAN
3 × 10^9 L
5 × 10^5 L E.O.
I.G. = 0.4 mA
7 × 10^6 L E.O.
I.G. = 4 mA
N(E) (arb. units)
130
20
10
0
BINDING ENERGY (eV)

Fig 6a

APPENDIX B

In Press - J. Vac. Sci. and Tech. Oct./Nov. 1981

COLUMN 3 AND 5 ELEMENTS ON GaAs (110): BONDING AND ADATOM-ADATOM INTERACTION*

Perry Skeath, C. Y. Su,
I. Lindau, and W. E. Spicer
Stanford Electronics Laboratories
Stanford University
Stanford, California 94305

---

*Supported by the Advanced Research Projects Agency of the Department of Defense and monitored by the Office of Naval Research under Contract No. N00014-79-C-0072 and by the Office of Naval Research, ONR N00014-75-C-0289. Part of the work was performed at SSRL which is supported by the National Science Foundation, NSF DMR77-27489, in cooperation with the Stanford Linear Accelerator Center and the Department of Energy.

Abstract

Column 5 elements adsorbed on GaAs (110) exhibit strikingly different behavior than adsorbed column 3 elements in terms of the overlayers bonding to the semiconductor, effect on the semiconductor surface lattice, and long-range order. A strong interaction between adatoms is found with submonolayer coverings of column 3 metals which leads to the formation of flat raft-like metallic patches. Unlike the column 3 metals, Sb adsorption produces large changes in the electronic states and atomic arrangement of the semiconductor surface lattice. An elementary view of the factors responsible for the different characteristics and effects of these overlayers on GaAs (110) is given, but its extension to other adatoms is shown to be limited.

These results have strong relevance to current theoretical models of Al and Ga overlayers on GaAs (110), as well as to molecular beam epitaxy and Schottky-barrier formation.

I. Introduction

Metal-semiconductor interfaces have attracted increasing amounts of interest recently. These interfaces are of obvious practical importance in determining the characteristics of ohmic and rectifying contacts to semiconductors. Of particular interest here are the microscopic interactions which occur at the interface [1] since it is thought that some important junction characteristics, such as interdiffusion or reaction of the metal and semiconductor [2], or Schottky-barrier height [3], are controlled by these interactions.

Such interactions are also important in the epitaxial growth of semiconductors using molecular beam epitaxy (MBE) techniques. It has been demonstrated that the characteristics of the epitaxial layer are strongly affected by surface conditions during growth. Examples of this include control of the lattice site occupied by dopant atoms [4] and the type of defects incorporated in the lattice [5].

We have used ultraviolet and soft X-ray photoemission spectroscopy (UPS, XPS) and low energy electron diffraction (LEED) techniques to investigate the bonding of column 3 and 5 elements on GaAs (110) and the effect of that bond on the semiconductor surface lattice reconstruction and electronic states. The column 3 overlayer data [6,7] is summarized and discussed first. The study of Sb overlayers is presented and discussed in more detail and comparison made to the behavior of column 3 metals on GaAs (110) as well as to the results of other workers.

II. Experimental Considerations

This investigation was done using continuously-variable nearly monochromatic light (40 eV $\lesssim h\nu \lesssim$ 500 eV) from the 4° beam line and

(10.2 eV $\lesssim h\nu \lesssim$ 32 eV) from the 8° beam line at the Stanford Synchrotron Radiation Laboratory [8] and a standard UHV system. The GaAs crystals used were nearly degenerately doped p-type (2×10^{18} cm^{-3} Zn, Laser Diode) or n-type (5×10^{17} cm^{-3} Sn, Varian). Clean GaAs (110) surfaces were prepared by cleaving under vacuum. Surfaces with low defect density are produced by this technique [9,10]. Synchrotron radiation was incident on the GaAs surface at an angle of 14°, and a PHI 15-255G double-pass CMA with axis normal to the (110) surface was used for photoelectron energy analysis. The CMA accepts electrons in a polar angle window of 42.3° ± 6° and essentially all azimuthal angles. Metal deposition was accomplished by evaporating from a shuttered bead or quartz crucible source and thickness determined by a Sloan crystal thickness monitor. The metal sources and deposition techniques are described in more detail elsewhere [6]. We define monolayer (ML) coverage to be 0.89×10^{15} *atoms/* cm^2--the same as the number of atoms in the surface lattice of GaAs (110)--*for convenience*. Exposures of GaAs to Sb are given in terms of a dosage (in units of 10^{15} atoms incident/cm^2) instead of coverage due to a varying sticking coefficient of Sb on GaAs. These dosages are determined by referencing to an Sb-covered thickness monitor and thus assume a unity sticking coefficient for Sb on Sb. Thus, relative dosages are well determined, but the absolute dosages may be in error by a factor equal to the reciprocal of the sticking coefficient of Sb on Sb. The error is probably less than a factor of two or three, based on a comparison of the Sb on GaAs data to similar data from clean cleaved GaSb taken during the same experiment.

LEED I-V data were obtained using a standard Varian four-grid LEED optics (shielded by mu-metal) and a Gamma Scientific T-5 spot photometer.

Only a single scan of each spot was done; thus, the gross features of each I-V curve are reliable although the details are probably not accurate.

III. Summary of Results and Discussion of Column 3 Metal Overlayers

Detailed results of the deposition of Al and Ga on GaAs (110) have been given elsewhere [6,7,11] and are outlined here with discussion to facilitate comparison to the column 5 element (Sb) results.

Increasing deposition of Ga on GaAs (110) produced a uniform attenuation and rigid shift (due to Fermi-energy pinning) of the semiconductor valence-band EDC features with no other change of those features [7]. Difference curves were taken to examine the effect of Ga adsorption on the semiconductor's surface electronic structure in more detail (see Fig. 1). The striking similarity of the UPS difference curves at submonolayer Ga coverage to the bulk (10 ML) Ga curve immediately suggests the formation of large three-dimensional Ga clusters or balls on the GaAs surface. However, previous analysis given elsewhere [7] has pointed out that this is inconsistent with the constant final state (CFS) and UPS data when taken as a whole. To summarize, the strong attenuation of the excitonic transition at $\geq$0.5 ML coverage together with the lack of perturbation of the GaAs EDC structure by Ga adsorption led to a model in which the Ga is distributed across the surface two dimensionally.

The metallic nature of the Ga overlayer (seen in Fig. 1) is worth examining in detail, since this gives information on how the Ga bonds to the surface. Positioning of a single Ga adatom within the surface unit cell--the usual model employed in calculations--gives an odd number of electrons within the cell and thus a metallic structure. However, calculations which use a model in which the Ga (or Al) adatom is constrained

to a specific binding site within the surface unit cell also give strong, sharp peaks in the local density of states at the surface [12,13,14] in sharp contrast to the observed free-electron-like difference curves obtained from the UPS data at comparable or lower coverages (see Fig. 1). In view of this observation, it seems necessary to include bonding between adatoms in order to account for the free-electron-like structure. It has been pointed out that the inclusion of interaction between adatoms in the calculations using one Ga (or Al) per unit cell does broaden out the calculated states [15]. However, the matrix elements between adatoms which one might use to broaden the calculated adatom states decrease proportional to the square of the distance between adatoms near equilibrium and fall off exponentially for separations far from equilibrium [16] ($\gtrsim$4 Å between adatoms for one adatom per surface unit cell, compared to a nearest neighbor distance of ~2.5 Å in GaAs). Thus, it seems unlikely that interactions at such large distances could account for the free-electron-like structure seen at low ($\lesssim$0.5 ML) coverage in the difference curves.

We, thus, consider a model in which the Ga adatoms are much closer together, allowing bonds to form between adatoms which are comparable in strength to the adatom-substrate bonds. This model has the advantage that at low ($\lesssim$0.5 ML) coverage the lowest energy configuration of the Ga adatoms will be two-dimensional raft-like patches (not necessarily ordered) consistent with the constant final state data and having a free-electron-like electronic structure consistent with the UPS difference curves. It should be mentioned here that the Ga-Ga (adatom-adatom) interaction which we discuss here is unrelated to the Ga-Ga (adatom-substrate) interaction discussed by Chadi et al [13].

A further result obtained from the data is that the bonding between the adatoms and substrate is mainly nondirectional. At submonolayer coverage, the Ga atoms in the overlayer come close enough together to form metallic bonds and yet bind to the semiconductor without major changes in GaAs surface lattice structure (as evidenced by the lack of change in EDC structure associated with the GaAs surface lattice). If the bond between Ga adatom and GaAs substrate were directional, as has been implied by other workers [12,13], the adatom would take a specific site within the surface unit cell, in which case a metallic bond between adatoms would most likely not form at low coverages ($\leq$0.5 ML) due to the large distance ($\geq$4 Å) between adatoms on adjacent sites. If, on the other hand, we allow the adatoms to come together to form two-dimensional rafts and then form directional bonds to the substrate, there would most likely be a significant mismatch and strain between overlayer and substrate which could cause smearing of EDC structure associated with the GaAs surface lattice. This effect is not seen, and thus the bond between Ga and GaAs is not very directional. This conclusion is supported by observations of LEED patterns before and after ~0.4 ML of Al deposited on GaAs (110), in which a lack of evidence for long-range order in the overlayer or change in surface lattice reconstruction was noted by a lack of change in relative spot intensities at the several beam energies examined.

Some discussion of other workers results is useful here. In supporting the calculations using tight binding models [12,13], reliance has been placed on Ga- or Al-induced peaks seen in soft XPS valence-band data [17]. However, the induced peaks are weak compared to the free-electron-like emission seen in that data. Thus, the overall trend is for the adatom-adatom interaction to lead to the formation of two-dimensional rafts,

probably without long-range order. It has been suggested that some atoms in the metallic rafts may tend to be "anchored" or bonded to the semiconductor at specific sites, possibly bonding to the Ga atoms in the semiconductor surface lattice [18]. The bonding states associated with the anchoring site could give rise to weak EDC structure such as that seen by Bachrach [17].

van Laar et al [19] have observed changes in the "As dangling bond" state seen in their AREDC spectra following deposition of Al or In. The UPS data shown in Fig. 1 was integrated with respect to azimuthal angle and, as discussed above, the lack of change in GaAs-derived EDC structure indicates that the GaAs surface lattice electronic structure was not strongly perturbed by the Ga overlayer. However, the angle-resolved UPS data of van Laar et al indicate that the detailed character of the surface states was changed by the Al or In, although the source of these changes (bond formation, loss of translational symmetry, or otherwise) is not yet understood. Further work is under way to understand the cause of this apparent difference.

IV. Results: Column 5 Element Overlayer

Adsorption of antimony (Sb) on GaAs was studied by soft X-ray photoemission spectroscopy (SXPS) as increasing exposures of the surface to Sb were made (see Fig. 2). Ga-3d, Sb-4d, and As-3d core levels as well as the valence band were monitored. At low dosages ($\lesssim 0.15 \times 10^{15}$ cm^{-2}), emission from the Sb 4-d core levels is extremely weak and no change is evident in the semiconductor core levels and valence band (except for a rigid shift indicating a quarter-volt increase in band bending after the second exposure). The amplitude of the Sb-4d emission after dosage of

0.14×10^{15} cm^{-2} is only one-fifth of the amplitude expected with a "unity" sticking coefficient (see experimental section). Emission from the Sb-4d core level increased dramatically after a total dose of 0.4×10^{15} cm^{-2}, suggesting that the sticking coefficient of Sb on this surface had increased after the first two exposures.

NO P

Changes in Ga- and As-3d core level widths are $\lesssim 0.15$ eV throughout the Sb deposition. The valence-band emission resembles a superposition of bulk Sb emission on GaAs at a dosage of 1.4×10^{15} although some differences, particularly near the valence-band maximum, are apparent. At high coverages ($>7 \times 10^{15}$ dosage), the Sb-4d spin orbit splitting is much better resolved although no appreciable ($\gtrsim 0.2$ eV) broadening or shifting of the Sb-4d core level as a whole was observed as a function of exposure.

The valence-band emission was given a more detailed examination using ultraviolet photoemission spectroscopy (UPS). The as-cleaved surface of n-type GaAs exhibited some broadening or smearing of valence-band structures, indicative of nonuniformity of strain or small variations in Fermi-energy pinning (initially pinned near 0.8 eV above the valence-band maximum) at the surface [9,10] (see Fig. 3). As with many other adsorbates, a small amount ($\lesssim 0.1 \times 10^{15}$ cm^{-2}) of Sb improved the EDC structure sharpness [6]. Low dosages of Sb, up to 0.3×10^{15} cm^{-2}, had little effect on the EDC structure beyond the sharpening observed with the first dose and no effect on the surface Fermi energy (E_{FS}). However, an increase of the total dosage to 1.0×10^{15} cm^{-2} resulted in the abrupt appearance of a

new peak 1.5 eV below the valence-band maximum (VBM) seen at all photon energies which were used ($h\nu$ = 18, 21, and 30 eV). This is consistent with the Sb uptake characteristics seen in Fig. 2. The GaAs peak at -2 eV ($h\nu$ = 21 eV) apparently disappears at the same time.

No P

Further deposition of Sb results in the attenuation of the new peak (-1.5 eV) and GaAs EDC structure by the bulk Sb valence band.

A single deposition of Sb was made on a p-type surface which had very sharp EDC structure (see Fig. 4) to eliminate the complication of the structure sharpening effects [6] seen above. Following a dosage of 1.5×10^{15} cm^{-2} Sb, the appearance of the peak -1.5 eV below the GaAs VBM and disappearance of the -2 eV peak is seen clearly. E_{FS} shifted from 0.2 eV to 0.5 - 0.6 eV above the VBM as a result of Sb deposition.

No P

The difference curve (Fig. 4) bears strong resemblance to the bulk Sb (noncrystalline) EDC except for the deep notch at -2 eV due to the loss of the GaAs EDC peak at that position.

The LEED pattern was observed before and after dosing of another GaAs (110) surface with 1×10^{15} cm^{-2} Sb. A 1 × 1 symmetry was preserved after Sb adsorption, and the background level remained the same (or even decreased at higher primary energies). A 1 × 1 symmetry was also preserved after Al adsorption (~0.4 ML) but with a substantial increase in background, consistent with a lack of long range order in the overlayer. I-V data were obtained for the $(\bar{1}0)$, $(\bar{1}\bar{1})$, and $(\bar{1}1)$ beams before and after Sb deposition (see Fig. 5). Changes in the relative spot intensities

are readily apparent. In some cases, strong peaks seen from the clean surface are wiped out after adsorption of Sb, and new strong peaks can be seen where very little intensity was observed on the clean surface. Thus, the binding of Sb to a specific site (or sites) within the GaAs surface unit cell and a major change in the reconstruction of the GaAs surface lattice is suggested by the I-V data. A more complete investigation of Sb overlayers on GaAs (110) by LEED I-V techniques is planned.

V. Discussion

The behavior of Sb on the GaAs (110) surface was, in most ways, completely different from the column 3 elements. Of particular importance was the effect of Sb adsorption on the GaAs (110) surface lattice electronic structure, in which a peak at -2 eV was removed (see Fig. 4). This suggests that partial rehybridization of surface or second-layer orbitals and a corresponding new reconstruction of the GaAs surface lattice has been forced by the bonding of Sb to the surface. It is interesting to note that both pseudopotential [21] and tight binding [22] calculations of states associated with the clean reconstructed GaAs (110) surface have indicated only back-bond or second-layer states near this energy. The LEED I-V data are consistent with this model since one monolayer of Sb was sufficient to completely change the I-V curves (although the pattern symmetry remained the same), wiping out several peaks characteristic of the clean reconstructed surface. Several of these peaks which disappeared were at primary beam energies between 150 and 250 eV, where the inelastic scattering length [23] is on the order of 10 Å, thus, contributions from below the surface layer can be significant. However, new multiple scattering effects or phase shifts due to the ordered

adatoms can contribute to the shift or disappearance of these peaks and, thus, attenuated peaks characteristic of the clean reconstructed surface may or may not be observable if the reconstruction was unchanged. Although very suggestive of a change in surface lattice reconstruction, further determination of the I-V data and comparison with calculations is desirable.

Referring back to the UPS data, the fact that the -2 eV state is relatively stable with respect to Ga deposition is then significant evidence for a lack of a major change in GaAs (110) surface lattice reconstruction by column 3 metals. The large changes in reconstruction due to column 3 metal adsorption which are predicted by tight binding calculations [12,13] may be due to the specific models chosen for those calculations. It would be particularly useful to know the effect of a free-electron-like (jellium) overlayer on the GaAs (110) reconstruction. However, to the authors' knowledge, no such calculation has been published.

In addition to the changes in the GaAs-derived features in the valence-band EDCs, a Sb-induced peak was observed at 1.5 eV below the GaAs valence-band maximum (VBM). UPS data ($h\nu$ = 18, 21, and 30 eV were used) revealed that the peaks position and amplitude were fairly constant with respect to the GaAs valence band. Strong emission was also observed at this peak position in the soft XPS valence-band EDCs (see Fig. 2, $h\nu$ = 90 eV), although the poor resolution (~0.5 eV) used for those valence-band spectra did not allow clear observation of the peak. Thus, the state associated with this peak is probably atomic-like, having no apparent amplitude variations or dispersion which would be expected of band-to-band transitions.

van Laar et al [19] have also studied N, P, and As on GaAs (110) using angle-resolved UPS but did not report the removal of any surface-sensitive states and saw only minor adsorbate-induced EDC structure. Different experimental procedures may help account for this discrepancy [7].

The less well-defined spin orbit splitting of the Sb-4d core level from submonolayer coverage up to several monolayers does suggest that Sb atoms are found in more than one (nonequivalent) site on the surface

(lifetime shortening effects are not expected here). At low coverages ($\theta \lesssim 0.5$ monolayer), the possibilities include bonding of two or more atoms at different sites within the surface unit cell or adsorption of a fraction of the Sb in molecular form. In the one-half to three monolayer range, there are necessarily different sites which are occupied until, at high coverages, the bulk Sb contribution is dominant and the spin orbit splitting well resolved.

The ordering of the Sb overlayer and the lack of long-range order of the column 3 metal overlayers suggests a fundamental difference in the type of bond between adsorbate and semiconductor for the two cases. The bond between Sb and the GaAs (110) is undoubtedly highly directional (covalent), whereas we see no evidence for a directional bond between Al or Ga and the semiconductor. Mrstik et al [24] and Kübler et al [25] have reported ordering of As on GaAs (110) with a (1×1) LEED structure, and thus the ordering of column 5 elements on GaAs (110) is not limited to Sb. Unlike Sb, deposition of As up to 1 ML results in a strong increase in the background seen in LEED [25], perhaps due to a greater tendency for As to remain in molecular form compared to Sb. The interaction between column 5 atoms (or molecules) bonded to the GaAs surface lattice is expected to be less significant than for the column 3 metals, since the adatom-adatom interaction was at the basis of the lack of registry between column 3 metal overlayer and GaAs (110) surface lattice in the two-dimensional raft model. The lack of directionality in the column 3 metal to GaAs (110) bond is probably related to the metal's predominately s-like valence and, conversely, the more p-like valence of the Sb is expected to result in more directional bonds.

It is interesting to note that the GaAs (110) surface accomodates both types of bonds. This is accomplished without a major change in surface reconstruction for column 3 metal overlayers, but the surface lattice is strongly affected by column 5 elements (Sb, as shown above, and As in Refs. 24 and 25). It is not surprising that a change of hybridization within the GaAs (110) surface lattice would occur as a result of covalent bond formation to an overlayer. However, the basis for the apparent lack of change in the reconstruction when column 3 elements are adsorbed is less obvious. Theoretical understanding of the effects on the surface lattice (both electronic and structural) of bond formation to an overlayer with s-like valence would be of great interest here.

In a simple picture taken from the above discussion, the ordering of the overlayer is determined by the directionality of the bond to the semiconductor and the attractive interaction between adatoms. A few examples (restricted to GaAs), however, will suffice to show that this elementary view is not always sufficient. Al has been observed to grow epitaxially on the (001) surface of GaAs, most likely due to a very good lattice match between the GaAs (001) and the Al (001) crystal faces [26, 27]. Alkali metal overlayers are an interesting case in which the adatom-adatom interaction is expected to be repulsive [28] and thus influence the ordering of Na [29] and Cs [30] on GaAs (110). Thus, ordering may occur even with atoms having only s-like valence electrons due in part to the interaction between adatoms. Fe can be grown epitaxially on GaAs (100), again probably due to the close lattice matching [27]. In the above scheme, oxygen would very likely form an ordered overlayer (assuming insignificant interaction between oxygen adatoms). However, oxygen adsorption has been found to <u>disorder</u> the surface lattice of GaAs (110)

[311, possibly by distortions associated with strongly localized O-As and O-Ga bonds [32].

Acknowledgement

The authors are indebted to the Tube Lab for their assistance with modification of the UHV equipment and to the SSRL staff for their technical support. M. Hecht contributed much of the data aquisition software, and Dr. J. Miller assisted with the LEED I-V measurements.

References

1. J. M. Andrews and J. C. Phillips, Phys. Rev. Lett. 35, 56 (1975).

2. G. Ottaviani, J. Vac. Sci. Technol. 16, 1112 (1979).

3. I. Lindau, P. W. Chye, C. M. Garner, P. Pianetta, C. Y. Su, and W. E. Spicer, J. Vac. Sci. Technol. 15, 1332 (1978); P. W. Chye, I. Lindau, P. Pianetta, C. M. Garner, C. Y. Su, and W. E. Spicer, Phys. Rev. B 18, 5545 (1978).

4. A. Y. Cho and I. Hayashi, J. Appl. Phys. 42, 4422 (1971).

5. J. H. Neave, P. Blood, and B. A. Joyce, Appl. Phys. Lett. 36, 311 (1980).

6. P. Skeath, I. Lindau, P. W. Chye, C. Y. Su, and W. E. Spicer, J. Vac. Sci. Technol. 16, 1143 (1979).

7. P. Skeath, I. Lindau, C. Y. Su, P. W. Chye, and W. E. Spicer, J. Vac. Sci. Technol. 17 (in press).

8. S. Doniach, I. Lindau, W. E. Spicer, and H. Winick, J. Vac. Sci. Technol. 12, 1123 (1975).

9. P. Skeath, W. A. Saperstein, P. Pianetta, I. Lindau, W. E. Spicer, and P. Mark, J. Vac. Sci. Technol. 15, 1219 (1978).

10. P. Pianetta, I. Lindau, P. E. Gregory, C. M. Garner, and W. E. Spicer, Surf. Sci. 72, 298 (1978).

11. P. Skeath, I. Lindau, P. Pianetta, P. W. Chye, C. Y. Su, and W. E. Spicer, J. Electron Spectrosc. Relat. Phenom. 17, 259 (1979).

12. E. J. Mele and J. D. Joannopoulos, Phys. Rev. Lett. 42, 1094 (1979).

13. D. J. Chadi and R. Z. Bachrach, J. Vac. Sci. Technol. 16, 1159 (1979).

14. J. R. Chelikowsky, S. G. Louie, and M. L. Cohen, Solid State Comm. 20, 641 (1976).

15. J. D. Joannopoulos, private communication.

16. S. Froye and W. A. Harrison, Phys. Rev. B 20, 2420 (1979).

17. R. Z. Bachrach, J. Vac. Sci. Technol. 15, 1340 (1978).

18. W. A. Goddard, private communication.

19. J. van Laar, A. Huijser, and J. L. van Rooy, J. Vac. Sci. Technol. 16, 1164 (1979).

20. J. T. M. Wotherspoon, D. C. Rodway, and C. Norris, Philosophical Magazine B 40, 51 (1979); L Ley, M. Cardona, and R. A. Pollak, Topics in Applied Physics 27, 106 (Springer-Verlag, New York, 1979); J. C. Phillips, Bonds and Bands in Semiconductors, Academic Press, New York, 1973.

21. J. R. Chelikowsky and M. L. Cohen, Phys. Rev. B 20, 4150 (1979).

22. D. J. Chadi, Phys. Rev. B 18, 1800 (1978).

23. P. Pianetta, I. Lindau, C. M. Garner, and W. E. Spicer, Phys. Rev. B 18, 2792 (1978); I. Lindau and W. E. Spicer, J. Electron Spectrosc. Relat. Phenom. 3, 409 (1974).

24. B. J. Mrstik, S. Y. Tong, and M. A. van Hove, J. Vac. Sci. Technol. 16, 1258 (1979).

25. B. Kübler, W. Ranke, and K. Jacobi, Surf. Sci. 92, 519 (1980).

26. A. Y. Cho and P. D. Dernier, J. Appl. Phys. 49, 3328 (1978).

27. J. R. Waldrop and R. W. Grant, Appl. Phys. Lett. 34, 630 (1979).

28. R. L. Gerlach and T. N. Rhodin, Surf. Sci. 17, 32 (1969).

29. J. M. Chen, Surf. Sci. 25, 305 (1971).

30. A. J. van Bommel and J. E. Crombeen, Surf. Sci. 45, 308 (1974); Surf. Sci. 57, 109 (1976).

31. A. Kahn, D. Kanani, P. Mark, P. W. Chye, C. Y. Su, I. Lindau, and W. E. Spicer, Surf. Sci. 87, 325 (1979).

32. C. Y. Su, I. Lindau, P. W. Chye, P. R. Skeath, and W. E. Spicer, these proceedings.

Figure Captions

1. Difference curves for successively larger coverages of Ga on GaAs (110). The 10 ML difference curve is essentially the same as a "bulk" (~100 ML) Ga EDC at the same photon energy: weak emission (due to small cross section) from the Ga sp valence band between -2 eV and E_F, and a relatively strong back ground of Auger (MVV transition) and secondary electrons below -2 eV. The inset curves in the upper right-hand corner are taken from calculations by Mele and Joannopoulos [12] of the expected surface density of states with a column 3 metal atom bonded to each As atom in the surface lattice. The zero of energy is the semiconductor VBM.

2. Core-level ($h\nu$ = 110 eV) and valence-band ($h\nu$ = 90 eV) photoemission data for a sequence of Sb exposures on GaAs (110). Dosages are shown in units of 10^{15} incident atoms/cm^2 and, in some cases, the actual coverage is given in parentheses (10^{15} atoms adsorbed/cm^2) based on the ratio of areas under the Sb-4d and Ga-3d peaks and comparison to GaSb (110) EDCs. Note the increase in the degree to which the Sb-4d spin orbit splitting is resolved as the coverage is increased above a few monolayers. Relativistic dehybridization is probably responsible for the splitting of the Sb valence band [20].

3. Valence-band UPS data for a sequence of Sb exposures on GaAs (110). Dosages are given in units of 10^{15} atoms/cm^2.

4. UPS valence-band EDCs for clean and Sb-covered GaAs (110), along with a difference curve and "bulk" Sb EDC.

5. LEED intensity vs primary beam energy curves for the $(\bar{1}0)$, $(\bar{1}\bar{1}) = (1\bar{1})$, and $(\bar{1}1) = (11)$ diffracted beams on the clean and Sb-covered surfaces. A 1×1 pattern was observed in both cases. The 16-40 eV section of the clean $(\bar{1}0)$ beam has been reduced by a factor of four.

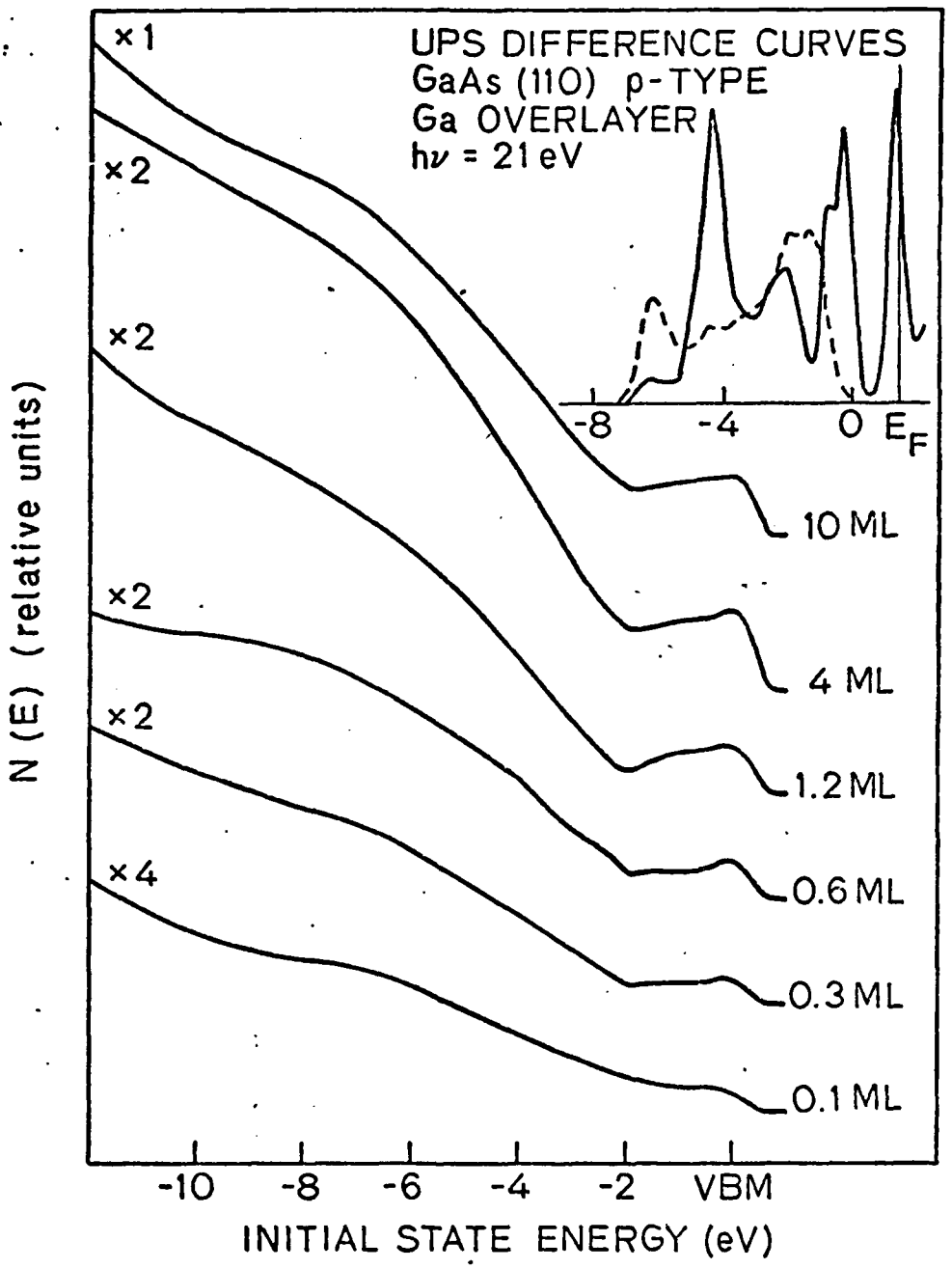
UPS DIFFERENCE CURVES
GaAs (110) p-TYPE
Ga OVERLAYER
hν = 21 eV
×1
×2
×2
×2
×2
×4
10 ML
4 ML
1.2 ML
0.6 ML
0.3 ML
0.1 ML
-8
-4
0
E_F
N (E) (relative units)
-10
-8
-6
-4
-2
VBM
INITIAL STATE ENERGY (eV)

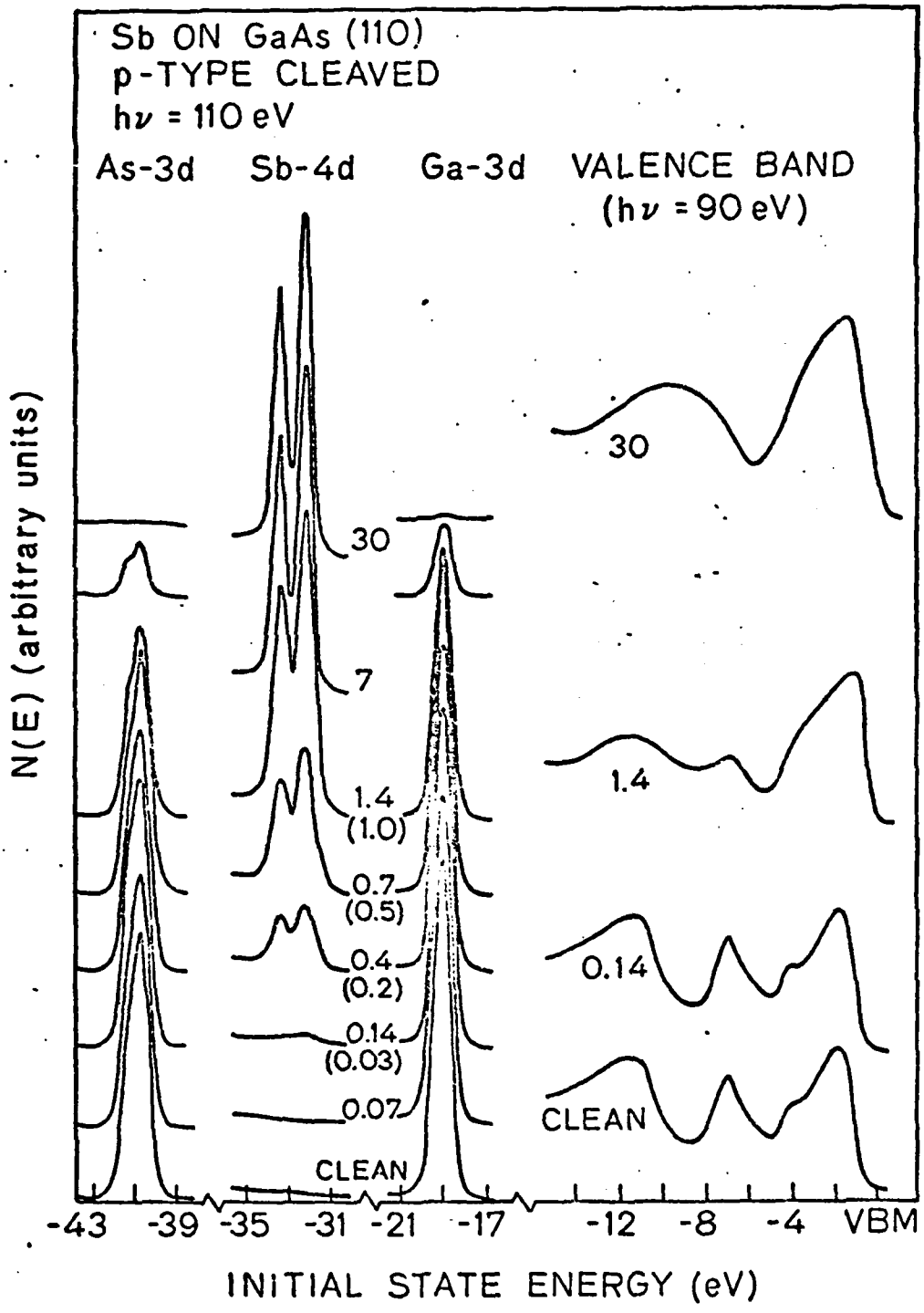
Sb ON GaAs (110)
p-TYPE CLEAVED
hν = 110 eV
As-3d
Sb-4d
Ga-3d
VALENCE BAND
(hν = 90 eV)
N(E) (arbitrary units)
30
7
1.4
(1.0)
0.7
(0.5)
0.4
(0.2)
0.14
(0.03)
0.07
CLEAN
30
1.4
0.14
CLEAN
-43
-39
-35
-31
-21
-17
-12
-8
-4
VBM
INITIAL STATE ENERGY (eV)

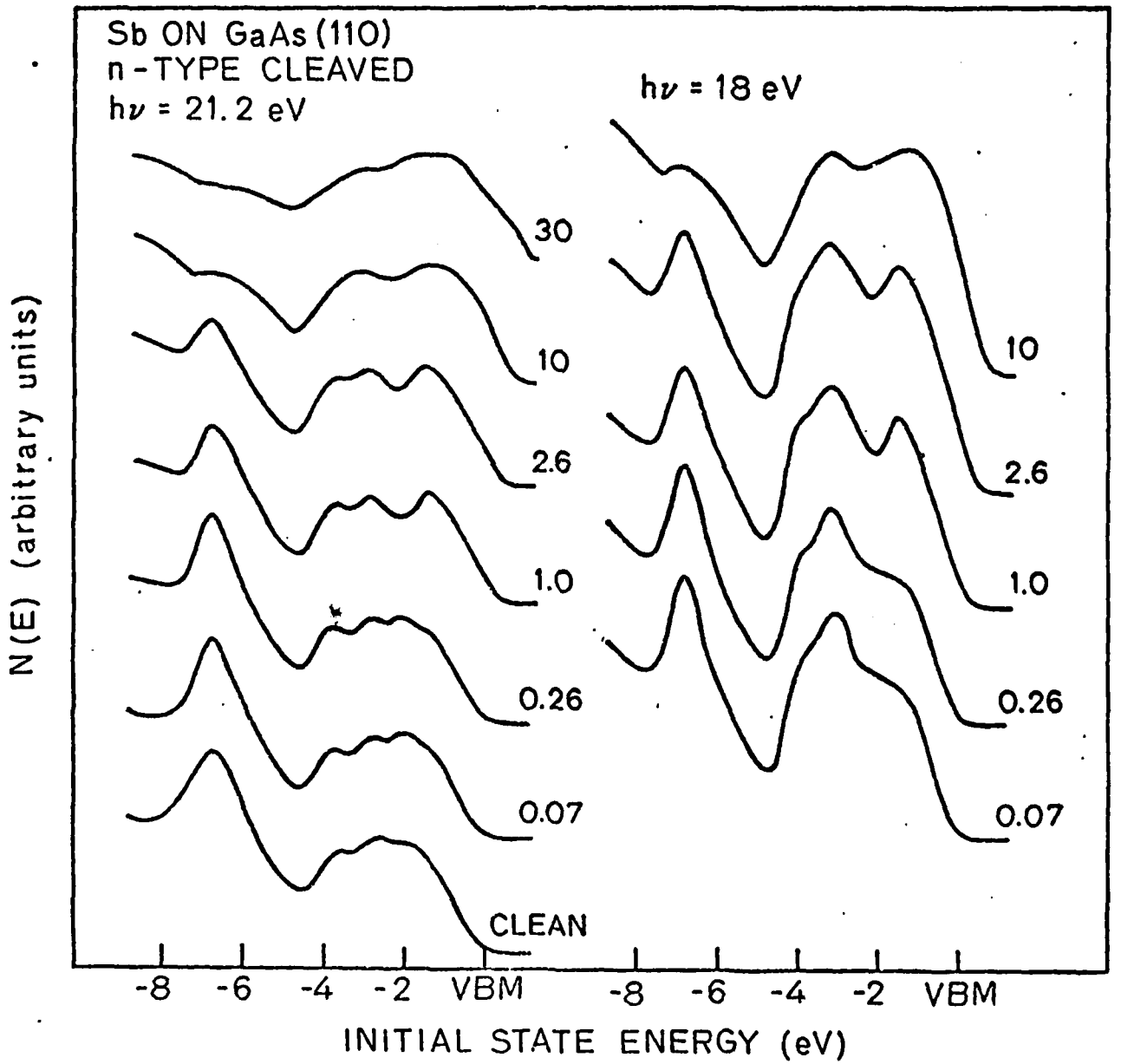
Sb ON GaAs (110)
n-TYPE CLEAVED
hν = 21.2 eV
hν = 18 eV
30
10
2.6
1.0
0.26
0.07
CLEAN
N(E) (arbitrary units)
-8 -6 -4 -2 VBM
-8 -6 -4 -2 VBM
INITIAL STATE ENERGY (eV)

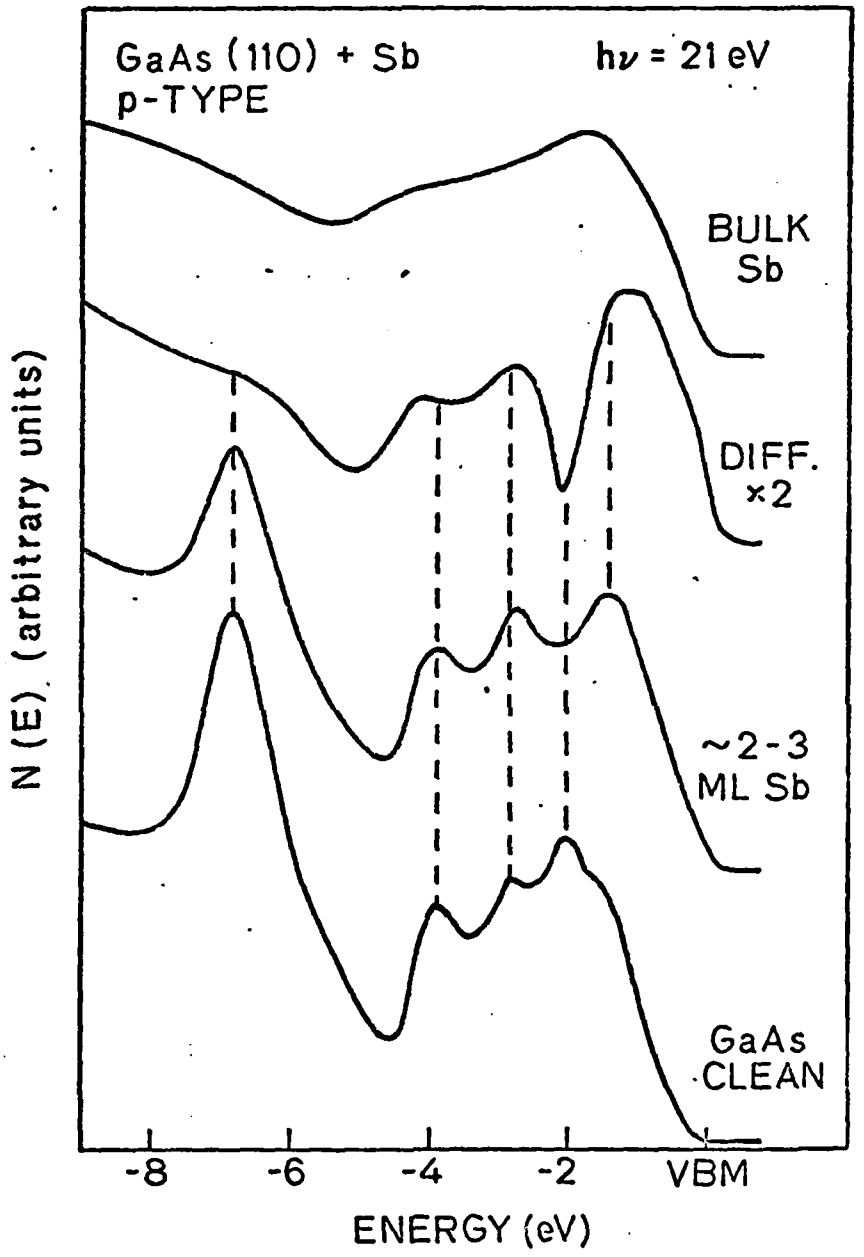
GaAs (110) + Sb
p-TYPE
hν = 21 eV
BULK
Sb
DIFF.
×2
~2-3
ML Sb
GaAs
CLEAN
N (E) (arbitrary units)
-8
-6
-4
-2
VBM
ENERGY (eV)

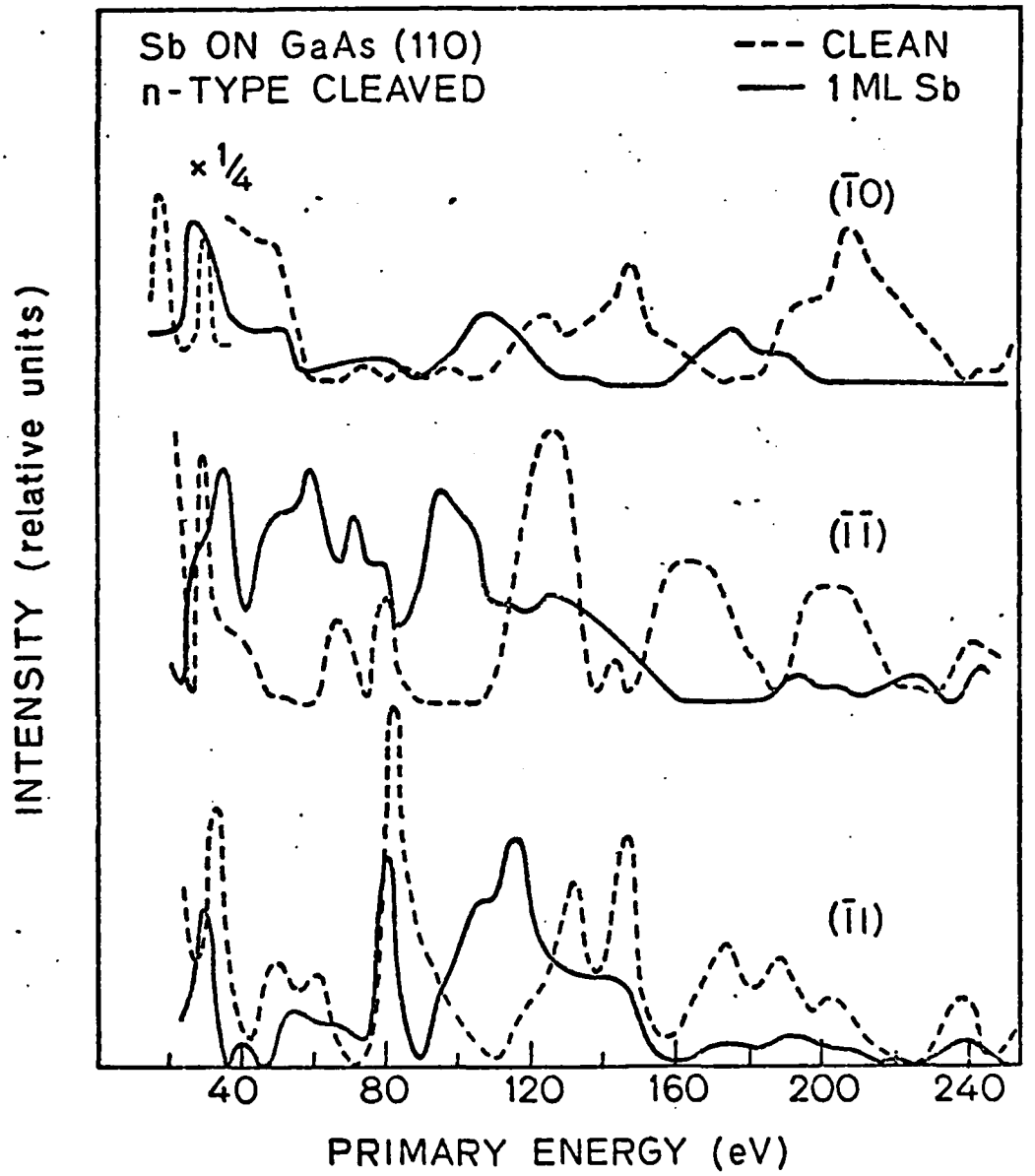
Sb ON GaAs (110)
n-TYPE CLEAVED
--- CLEAN
— 1 ML Sb
× 1/4
(1̄0)
(1̄1̄)
(1̄1)
INTENSITY (relative units)
40
80
120
160
200
240
PRIMARY ENERGY (eV)

APPENDIX C

In Press - J. Vac. Sci. and Tech. Oct./Nov. 1981

OXYGEN ADSORPTION ON THE GaAs (110) SURFACE

C. Y. Su, I. Lindau, P. R. Skeath,
P. W. Chye, and W. E. Spicer*

Stanford Electronics Laboratories
Stanford University
Stanford, California 94305, USA

Abstract

The adsorption of nonexcited molecular oxygen on cleaved GaAs (110) surfaces at room temperature has been studied using photoemission techniques. Detailed analysis of the oxygen-induced structure in the valence-band region revealed two different forms of adsorbed oxygen. Adsorption in the first form saturates at a very low coverage (~ 0.01 monolayer) and is probably associated with defect sites. Adsorption in the second form occurs at normal surface sites and produces measurable chemical shifts in Ga-3d and As-3d core levels. The nature of the second form of oxygen has been further investigated with core level studies of surfaces oxidized at room temperature and subsequently heated to a high temperature. Annealing to moderately high temperature ($\sim 370^{o}C$) causes transfer of oxygen from As-O bonds to form additional Ga-O bonds. Fast heating to high temperature ($430^{o}C \sim 450^{o}C$) leads to desorption of roughly half of the oxygen atoms and all of the chemically affected As atoms, while little change in the Ga-3d core level is observed. Several previously proposed oxidation models are compared based on the present data.

---

*Stanford W. Ascherman Professor of Engineering

1. INTRODUCTION

The problem of the interaction of oxygen with GaAs (110) surfaces has attracted much attention in the past few years (1-14). In particular, these studies have addressed the question of chemisorption sites and the question whether oxygen adsorbs nondissociatetively or dissociatively. Here we report two major findings which provide advances in answering these questions. In the valence band studies we have separated features due to two different adsorption states and thus clarified the previous use (1,7) of valance band region spectra for identifying atomic or "molecular" oxygen. In the core level studies, heat treatments of surfaces adsorbed with oxygen at room temperature have revealed many properties of the bonding between oxygen and substrate atoms.

Mele and Joannopoulos (MJ) (1) calculated the local density of states for various bonding schemes between oxygen and the surface atoms of GaAs (110). By comparing their results with the then available valence-band photoemission data, adsorption of molecular oxygen on the As of GaAs (110) was suggested. However, the only valence-band spectra (7) with good resolution available to them were taken with low energy photons ($\lesssim 21$ eV) where many oxygen-induced structures are shadowed by the secondary electron emission and suffer from low cross section. In this work, detailed analysis of the oxygen-induced structure is facilitated by using higher energy photons (30 eV) which gives increased cross section for oxygen and decreased cross section for the substrate and reduces scattered background. We found the features identified in Ref. 1 as molecular oxygen are of different nature and are unrelated to the major chemisorption state which produces the chemical shifts in Ga-3d and As-3d core levels. After separation of the features due to the two states, the spectrum for the

major chemisorption state is found to support the previous suggestion of dissociative chemisorption agreed upon among experimental groups (2,3).

Chemical shifts of Ga-3d and As-3d core levels were used more often in the past to answer the question of chemisorption sites (2,3,5). Agreement has been reached among experimental groups that there is an unresolved chemical shift of the Ga-3d level in addition to a well-resolved chemical of the As-3d level following oxygen adsorption (2,3). The interpretation of the chemical shift on the Ga-3d level, however, is not straightforward. Brundle and Seybold (3) have proposed the direct growth of Ga_2O_3 and As_2O_3, as the magnitude of chemical shifts are close to what is expected for these bulk oxides and the estimated stoichiometry indicated 1.4 oxygen atoms per chemically affected substrate atom. Pianetta et al (5) have suggested that AS-O bonding could induce broadening on the Ga-3d core level. Barton and Goddard III (4) have calculated an As-O bonding-induced chemical shift of 0.8 eV on the Ga-3d level as well as a 2.6 eV shift on the As-3d level. These shifts agree well with experiments (2,3,5). This divergence of interpretations illustrates the difficulty in attaining an unambiguous answer from the magnitude of the chemical shifts alone. The estimated stoichiometry can provide additional information with the limits of experimental uncertainties. In this work, we studied the changes on the core levels after heating room-temperature oxidized surfaces to various temperatures. We will show that idependent As-O and Ga-O bonding has to be invoked and, yet, it cannot simply be As_2O_3 and Ga_2O_3 with bulk properties.

2. EXPERIMENTAL

Experiments were performed in a standard stainless steel.ultrahigh

vacuum chamber with base pressure $\sim 10^{-10}$ torr (5). The light source used was synchrotron radiation from the 8° and the 4° beam lines of the Stanford Synchrotron Radiation Laboratory (SSRL) (6). The O-1s spectra were obtained with Mg-K emission ($h\nu$ = 1253.6 eV). Oxygen exposures were made with all the precautions necessary to avoid generating excited oxygen which could lead to different adsorption processes (5). The heating was achieved by radiation heating on the back end of the crystal from a tungsten filament enclosed with the molybdenum crystal holder. To avoid contamination during heating the heaters had been thoroughly outgased to temperatures $\gtrsim 500^{o}C$. Details of pressure changes in the vacuum chamber under different heating conditions will be indicated together with experimental results in Section 3.B. Temperatures were monitored with both a thermocouple mounted near the back end of the crystal and an infrared pyrometer focused near the crystal surface.

The difference curves were obtained from the energy distribution curves (EDCs) by consistently aligning both the Ga-3d peaks and the valence-band maxima of the EDCs. As there is no observable change on the Ga-3d core level for surfaces subjected to exposures smaller and equal to 10^6 L, the normalization was done by matching the Ga-3d amplitudes before substracting to obtain the difference curve. For surfaces subjected to exposures higher than 10^6 L, some changes are observed in the Ga-3d levels. In such cases, the substractions necessary for obtaining the difference spectra are done in such a way that zero intensity is reached at the energy position corresponding to the clean component of the Ga-3d level.

3. RESULTS AND DISCUSSIONS

A. Oxygen-Induced Structure in the Valence-Band Region

For GaAs (110) surfaces cleaved in situ and exposed to nonexcited molecular oxygen at room temperature, there are two qualitatively different exposure regimes observed in our previous studies. At or below 10^6 L (1 L = 10^{-6} torr-sec) exposure, there is no detectable change in either the As-3d peak or the Ga-3d peak (2,5,8), yet the Fermi-level has moved close to complete stabilization (7). Above 10^7 L exposure, there are definitely observable shifts on both the As-3d and the Ga-3d levels. The top two curves of Fig. 1 show the EDCs from a clean p-GaAs (110) surface and from the same surface expsosed to 10^6 L of oxygen. Even with this exposure in the low regime, the oxygen-induced structure in the valence-band region is highly visible at $h\nu$ = 30 eV. A comparison of the EDCs and the difference spectrum (the bottom curve in Fig. 1) clearly indicates the existence of four pieces of structure at binding energies (BE) of 4.6 $\pm$ 0.2, 5.8 $\pm$ 0.2, 7.8 $\pm$ 0.2, and 10.4 $\pm$ 0.2 eV.

The four oxygen-induced peaks can be divided into two groups according to their different rates of growth under increasing oxygen exposures. In Fig. 2, we show the EDC of a clean GaAs (110) (top curve) and the difference spectra of this surface subjected to a sequence of increasing oxygen exposures (the three center curves). Immediately apparent is the fast growth in strength of peak 1 (4.6 eV B.E.) in comparison to that of peak 4 (10.4 eV B.E.) in going from 10^5 to 10^7 L. The absolute strength of peak 4 stays approximately constant with increasing exposures showing that the oxygen state associated with peak 4 has already saturated. (This is further evidenced by the disappearance of intensity at the energy position of peak 4 in the bottom curve of Fig. 2, where we have substrated the 10^6 L

spectrum from the 10^7 L spectrum). Thus, for nonexcited oxygen adsorbed on GaAs (110) surfaces, there exist at least two different states of oxygen, one producing peak 4 which we shall designate as the first state and another one producing peak 1 which we shall designate as the second state.

Although the shadowing from the strong emission under peak 1 makes it more difficult to follow peaks 2 and 3 than peak 4, these two peaks appear to evolve similarly to peak 4 and hence are assigned to the first state. Peaks 3a and 3b are considered as small features of the second state. The finding of two oxygen states has also been reported by Ranke and Jacobi (9) for other surfaces (111 $\bar{1}\bar{1}\bar{1}$ 100) of GaAs. Their assignment of the peaks of the first form of oxygen is different from the present work. The concentration of the first form of oxygen is also invariably higher on the polar surfaces.

As the adsorption of oxygen in the first state saturates at exposure lower than 10^6 L, it is not related to the previously observed chemical shifts in the high exposure regime mentioned earlier. This immediately leads to clarification of the comparison made between experimental data and theoretical calculation in Ref. 1. The previous interpretation of the experimental spectra was done with inclusion of peaks in the EDC from two different forms of oxygen. It is the second state oxygen that is of relevance to Ref. 1. The bottom curve of Fig. 2 can be taken as a good representation of the spectrum for the second state oxygen. MJ (1) found three O_2-like molecular levels of comparable strength, with binding energies of 4, 8, and 10 eV. This group of multiple peaks is obviously not found in the bottom curve of Fig. 2. Rather, the spectrum showing a single dominant oxygen peak is indicative of dissociative chemisorption,

as discussed before. (1,2,3). The calculation also showed a shift towards higher BE (from 11 to 12 eV) of the As-4s-like band. This is taken as a signature for chemisorption of oxygen to the As. However, no structure can be found in the present spectra in the region with BE of 11 to 12 eV. Thus, we feel that MJ's theoretical results are not applicable to the second state of oxygen adsorption discussed here.

The intensity of emission from oxygen in the first state at 10^7 L is estimated to be less than 10 percent of that due to the second state. The oxygen coverage of the second state is estimated to be approximately 0.1 to 0.2 monolayer for a surface exposed to 10^7 L oxygen (2,5,8). Thus, the saturation coverage of the first state oxygen is approximately 0.01 ~ 0.02 monolayer. As explained in the introduction section, this low coverage of oxygen is detectable mainly due to a large difference in the strength of the matrix elements of the O-2p transition and the GaAs valence band transition. Here, by proper choice of photon energy, we have demonstrated the superior overlayer sensitivity that is achievable with the valence state photoelectron spectroscopic technique. We would estimate that coverages as low as 0.005 monolayer can be detected with this technique.

The low saturation on coverage reached with a low exposure suggests that the adsorption of the first state of oxygen may be at some type of surface defect sites. In contrast, adsorption of the second form oxygen continues to very high exposure, which obviously must occur on the normal surface sites of GaAs (110). Complete understanding of the nature of the first form of oxygen requires more studies. Considerations made on the relation between the two forms of oxygen can also lead to interesting

possibilities concerning the kinetics of oxygen adsorption on GaAs (110). These aspects of the present finding of two different adsorption states will be discussed elsewhere.

B. Effects of Heat Treatment of Oxygen-Covered Surfaces

In this subsection we address ourselves to the recurring question (2,3,4) of interpreting chemical shifts in the core levels which are caused by the adsorption of the second form of oxygen. We present new results obtained from heat treatment of surfaces adsorbed with oxygen at room temperature. Two qualitatively different types of heating conditions have been investigated. In the first, temperature was brought up from room temperature to 350°C ~ 370°C and annealed for 30-40 minutes. The chamber pressure increased only slightly at the beginning of annealing and remained stable during annealing. The major effects of annealing are reproducibly observed on several surfaces.

In Fig. 3a and 3b, we show, respectively, the As-3d and Ga-3d core levels of GaAs (110) surface exposed to $10^{10}LO_2$ ($\theta \approx 0.6$) at room temperature and then annealed at 370°C for approximately 30 min. The spectra are normalized to have equal height for the unshifted As-3d peaks. The sharp decrease (by a factor of ~6) in the intensity of the shifted As-3d (fig. 3a) and the increase in the broadening toward high BE of the Ga-3d level (fig. 3b) are clear. Also apparent is the increase in the ratio of total intensity of Ga-3d to As-3d. (This ratio is not affected by the normalization). The decrease in the intensity of shifted As-3d approximately equals the decrease in the total intensity of the As-3d.

Thus some of the surface As atoms bonded to oxygen after room temperature adsorption are lost from the surface during annealing. On the other hand, the O-1s intensity is seen in fig. 3c to show no detectable change after annealing, indicating that no desorption of oxygen has occurred during annealing. The changes in the chemically shifted Ga-3d and As-3d levels can be interpreted as due to transfer of oxygen in As-O bands to form additional Ga-O bonds, with conservation of the total number of oxygen atoms on the surface. The loss of As from the surface is suggestive of the formation of the stable oxide, Ga_2O_3, because the participation of a surface Ga in forming Ga_2O_3 requires breaking of all bonds to its neighboring surface As, which in turn makes the release of some As easier. The lack of sudden pressure rise in this annealing process, as contrasted to a sharp pressure rise detected in the fast heating process to be discussed below, is also consistent with the above proposal, because to release a monolayer of As in 2000 sec gives a pressure rise only about 5×10^{-10}torr which is smaller than the background pressure during annealing ($3\text{-}4 \times 10^{-9}$torr).

The result of having oxygen transferred from As-O bonds to form Ga_2O_3 is expected from the thermodynamics governing the three elements: O, Ga, and As. However, the fact that it is necessary to supply heat to have the thermodynamic predictions prevail, reflects that room temperature adsorption results in an intermediate metastable chemisorption phase which is separated from the chemically most stable compounds by an activation barrier. The activation barrier can be, for example, breaking of the GaAs back bonds. Since the formation of Ga_2O_3 and As_2O_3 requires breaking of all GaAs back bonds, it is difficult to see, if Ga_2O_3 and AsO_3 can indeed be formed by room temperature adsorption, that there should be

any additional barrier against forming predominantly Ga_2O_3 at room temperature. In general, for selecting possible models for adsorption on solid surfaces, the important consideration is often not the total energy, but is the activation energy. The present annealing data show that the room temperature adsorption of oxygen on Ga As (110) surface is governed by the activation barrier, i.e., the chemisorption phase is quite different from the most stable oxides.

In fig. 3d we show the variation of vapor pressure with temperature of the two crystalline forms of As_2O_3 (11). This curve indicates high volatility of As_2O_3 at all temperatures above room temperature. In particular, by using the extrapolated value of vapor pressure at 370°C and an unusually low evaporation coefficient (10^{-7}), an evaporation rate of $7,5 \times 10^{15}$ molecules/cm^2-sec is found (12). With this evaporation rate, it requires only 0.1 second to evaporate a monolayer (10^{15} molecules/cm_2) of As_2O_3. If the chemically shifted As-3d were to be interpreted as due to As_2O_3, it would be tempting to explain the absence of desorption of oxygen by strong competition of the transformation of arsenic oxides into gallium oxides with the evaporation of arsenic oxides. However, the chemically shifted As-3d did not disappear completely (fig. 3a) after holding the sample at 370°C for 30 minutes. The chemically shifted As-3d remained after annealing has about one sixth of the orginal intensity, it is hard to explain why this significant amount of As_2O_3 which escaped transforming into Ga_2O_3 by heating can stay on the surface without being evaporated away. The interpretation of the chemical shift in As-3d as due to As_2O_3 is thus considered highly improbable.

In the other type of heat treatment, a relatively fast heating rate ($\geq$ 5°C/min between 300°C and 450°C) was used to bring the temperature to

$\geq$430°C. Heating was terminated after a sharp pressure rise ($\sim 10^{-7}$ torr for 2-3 sec over a background pressure of $3 \sim 4 \times 10^{-9}$ ton, as monitored by a cold cathode gauge). Although no mass-spectrometric measurement was done, the photoelectron spectroscopic measurements of the resulting surfaces indicate that, as will be detailed below, the sharp pressure rise could well be correlated to desorption of As and oxygen from the sample surface, and did not correspond to any outgassing of other surfaces in the vacuum chamber. Such desorption has been observed on all surfaces subject to this type of heat treatment. However, in one case, substantial transformation of As-O bonds to Ga-O bonds was also observed. Complication arised from the mixed effects of the transformation and the desorption will be further studied in the future. In the other case, little transformation of As-O bonds into Ga-O bonds was observed to accompany the desorption. Results from this latter case give clear contrast to the results from the annealing experiment we just described, hence they will be discussed here.

In Fig. 4, we show core-level spectra of a GaAs (110) surface exposed to 10^9 L O_2 ($\theta \approx 0.5$) at room temperature and then heated at a relatively rapid rate to 430°C. The center curve in Fig. 4 shows the normally observed chemically shifted As-3d peak and the broadening on the Ga-3d peak after adsorption at room temperature (2,5). The spectrum taken after heating to 430°C shows complete disappearance of the shifted As-3d peak. But in contrast to the results shown in Fig. 3 there is only a slight increase in the broadening on the Ga-3d peak. The O-1s intensity, as shown in the inset of Fig. 4, decreased by a factor close to 2. The total intensity of As-3d decreased by approximately 25 percent which is equal to the percent shifted As-3d after adsorption at room temperature.

The decrease in intensity of O-1s and As-3d in conjunction with the pressure burst detected immediately prior to the termination of heating are strong indications of desorption of both oxygen and As from the surface. The slight increase in broadening on Ga-3d and the small deviation of the oxygen intensity ratio from 2 is attributed to a small amount of transformation of As-O bonds to Ga-O bonds that occurred before desorption. The drop of approximately a factor of 2 in O-1s intensity after desorption reinforces one point we have made previously--that is, there are equal amounts of shifted As-3d and Ga-3d at any coverage less than 1 monolayer (2).

A few previously proposed oxidation models can now be examined with information provided by the heating experiments. The model of direct growth of As_2O_3 and Ga_2O_3 is considered least likely among the models we will examine here. Although it can account for the presence of chemical shifts in both Ga-3d and As-3d core levels and it is consistent with the estimated stoichiometry. However, as discussed above, it contradicts the absence of complete desorption of the chemically affected As atoms at 370°C in a prolonged time duration.

In the simple chemisorption configuration suggested by ourselves (5) and theoretically studied by Barton et al (4), the chemical shift in the Ga-3d level is induced by oxygen atom chemisorbed to As. As mentioned earlier in the introduction section, this model can also explain the simultaneous shifts present in the Ga-3d and As-3d core levels, but the number of adsorbed oxygen atoms per surface Ga and As deviates from that estimated from experiments (3). To have this model account for the increase in the number of chemically affected Ga atoms after annealing,

it appears necessary to invoke bridge bonding of one oxygen atom to at least two Ga atoms. The same conclusion is reached in considering the results of the fast-heating experiment where after desorption the same number of chemically affected Ga atoms is to be produced by oxygen atoms only half of that is available before desorption. This type of oxygen-galium bonds, although it cannot be ruled out, is rather unusual. Therefore this model is also considered less likely to be correct. However, it is hoped that calculations of core level chemical shifts with other possible configurations will be carried out.

Ludeke (13) has proposed a model of oxygen bridging over surface Ga and As which is related to a distorted (111) layer of $GaAsO_4$ but $GaAsO_3$ in stoichiometry. This model can explain the presence of chemical shifts in both the As-3d and Ga-3d core levels. The surface stoichiometry is also close to that estimated from experimental data. In addition, this model offers the bonding configuration of a surface oxide phase which is characterized by reasonably strong bonding to the substrate. This last characteristic is consistent with the low volatility of the chemically affected As atom found in this work. The results of the 370°C annealing experiment can be explained by first breaking up the As-O bridge bonds in a $GaAsO_3$ unit with the resulted $Ga-O_3$ unit acquiring a neighboring Ga atom in the surface or in the second layer to form Ga_2O_3. In the fast-heating experiment, however, the temperature of the surface is raised high enough such that oxygen atoms in excess of forming Ga_2O_3 from two neighboring $GaAsO_3$ units desorb (perhaps as As_2O_3) before the GaO_3 units can acquire extra "free" Ga from the substrate. (We can write, for example, $GaAsO_3 \rightarrow As\uparrow + GaO_3$, $GaO_3 \rightarrow 1/2Ga_2O_3 + \frac{3}{4} O_2\uparrow$ or $2\ GaAsO_3$ $Ga_2O_3 + As_2O_3\uparrow$). While this explains the lack of change in the number

of chemically affected Ga atoms after half of the oxygen is desorbed away, it at the same time, implicitly assumes that the chemical shifts in the Ga-3d level caused by Ga_2O_3 and by Ga-O-As bridge bond are indistinguishable. This latter assumption, although it does not represent the simplest possible explanation for the lack of change in Ga-3d level after desorption, is not inconsistent with out present knowledge of the chemical shifts in Ga core levels. Overall, this model appears to be far more attrative than the two other models we considered above.

Before concluding, we want to introduce a simple model for future consideration. Namely, the model of simple chemisorption of one oxygen atom to each of the surface Ga and As without breaking all the back bonds. This model is consistent with all the important experimental observations made so far. It offers particularly simple explanation for the lack of change in the Ga-3d core level after fast-heating to desorption of oxygen and arsenic, by assuming preferential desorption of the As-O bonding units without disturbing the Ga-O bonding units. The weak point of this model may be its deviation from the estimated surface stoichiometry (number of oxygen atom per surface atom, 1 vs. ~ 1.4) (3).

4. SUMMARY

Two different forms of oxygen are found on GaAs (110) surfaces. Adsorption in the first form saturates at a low coverage (~0.01 monolayer) and probably occurs at defect sites. The second state of oxygen corresponds to the major adsorption state on this surface.

Core-level studies of heat-treated surfaces revealed new information about the nature of this chemisorption state. It is shown to be a surface chemisorption phase different from the stable oxides of this system. The surface chemisorption phase has to retain strong bonds to the substrate.

Ludeke's bridging oxygen bond model (13) is an example of such surface chemisorption phase and appears to be much more appealing than the other two existing models. A chemisorption model of one oxygen atom to each of the surface Ga and As is also introduced for future consideration, for its simplicity in explaining the present data of the heating experiments. It is hoped that further theoretical calculations will be carried out to test the various models.

ACKNOWLEDGMENT

Valuable discussions with W. Mönch are gratefully acknowledged. We also want to thank S. J. Oh and M. Hecht for assistance in experiments. This work was supported by the Office of Naval Research under Contract No. N00014-75-0289 and by the Advanced Research Projects Agency of the Department of Defense under Contract No. N00014-79-C-0072. The experiments were performed at the Stanford Synchrotron Radiation Laboratory which is supported by the National Science Foundation under Grant No. DMR77-27489 in cooperation with the Stanford Linear Accelerator Center and the Department of Energy.

REFERENCES

1. E. J. Mele and J. D. Joannopoulos, Phys. Rev. B 19, 6999 (1978); Phys. Rev. Lett. 40, 341 (1978); J. Vac. Sci. Technol. 15, 1287 (1978).
2. P. W. Chye, C. Y. Su, I. Lindau, P. R. Skeath, and W. E. Spicer, J. Vac. Sci. Technol. 16, 1191 (1979).
3. C. R. Brundle and D. Seybold, J. Vac. Sci. Technol. 16, 1186 (1979).
4. J. J. Barton, W. A. Goddard III, and T. C. McGill, J. Vac. Sci. Technol. 16, 1178 (1979).
5. P. Pianetta, I. Lindau, C. M. Garner, and W. E. Spicer, Phys. Rev. B 18, 2792 (1978); Phys. Rev. Lett. 35, 780 (1975); 37, 1166 (1976).
6. S. Doniach, I. Lindau, W. E. Spicer, and H. Winick, J. Vac. Sci. Technol. 12, 1123 (1975).
7. P. Pianetta, I. Lindau, P. E. Gregory, C. M. Garner, and W. E. Spicer, Surf. Sci. 72, 298 (1978).
8. I. Lindau, P. Pianetta, W. E. Spicer, P. E. Gregory, C. M. Garner, and P. W. Chye, J. Electron. Spectrosc. 13, 155 (1978).
9. W. Ranki and J. Jacobi, Surf. Sci. 81, 504 (1979).
10. The very low initial sticking coefficient on GaAs (110) of the second state oxygen (10^{-9}) and a nearly 10^6 times enhancement of this coefficient on a cesiated surface has led to the proposal of dissociation of oxygen molecules as the rate-limiting process for oxygen adsorption. C. Y. Su, P. W. Chye, P. Pianetta, I. Lindau, and W. E. Spicer, Surf. Sci. 86, 894 (1979).
11. O. Kubaschewski, Metallurgical Thermochemistry, 5th Ed., Oxford, New York, 1979.
12. Here we use the Knudson-Hertz equation to calculate the evaporation rate, $Rev = \alpha_v (p^*-p)/(2\pi mkT)^{1/2}$. In this equation α_v, the

evaporation coefficient, is the fraction of evaporant flux that makes the transition from condensed to vapor phase, p* is the vapor pressure of the evaporant. p is the hydrostatic pressure of the return flux. With $\alpha_v = 10^{-7}$, p* = 1 atm at T = 643°k. p* - p ≈ p*, we obtain Rev = 7.5×10^{15} molecules/cm^2-sec. As stated in the text, 1 monolayer of As_2O_3 can be desorbed in 0.1 second with this evaporation rate. For the ~0.065 monolayer of chemically affected As atom to survive heating at 370°C for 30 min, as is the case shown by Fig. 3a, α_v has to be smaller than 3×10^{-11} for the As_2O_3 interpretation to hold. Such small value of evaporation coefficient is not found to our knowledge. L. I. Maissel and R. Glang, Handbook of Thin Films, New York, 1970, Chap. 1.

13. R. Ludeke, Solid State Commun. 21, 815 (1977).

FIGURE CAPTIONS

1. EDCs of a clean p-GaAs (110) surface (top curve) and the same surface exposed to 10^6 L oxygen (center curve) taken at a photon energy of 30 eV. The bottom curve is their difference.

2. EDC of a clean N-GaAs (110) surface (top curve) and difference spectra of this surface subjected to step-increased oxygen exposures (center three curves). The bottom curve labeled 10^7 - 10^6 L is the difference between the EDCs of this surface exposed to 10^7 and 10^6 L of oxygen. Peaks 2, 3, and 4 are assigned to the first form of oxygen. Peaks 1, 3a, and 3b are assigned to the second form of oxygen.

3. The effect of annealing of a room temperature oxidized surface at 370°C for 30 min. Transfer of oxygen from As (panel a) to Ga (panel b) without losing oxygen (panel c) has been observed. However, some As leave the surface during annealing, possibly as a result of forming Ga_2O_3 (see text). For reference, panel (d) indicates the vapor pressure of the two forms of As_2O_3.

4. The effect of fast-heating of a room temperature oxidized surface to ~430°C. In contrast to the effect of annealing at 370°C (fig. 3), a decrease of about a factor of 2 is seen in the O-1s intensity (inset) and the shifted As-3d peak disappeared without appreciable change in either the unshifted As-3d peak or the Ga-3d peak.

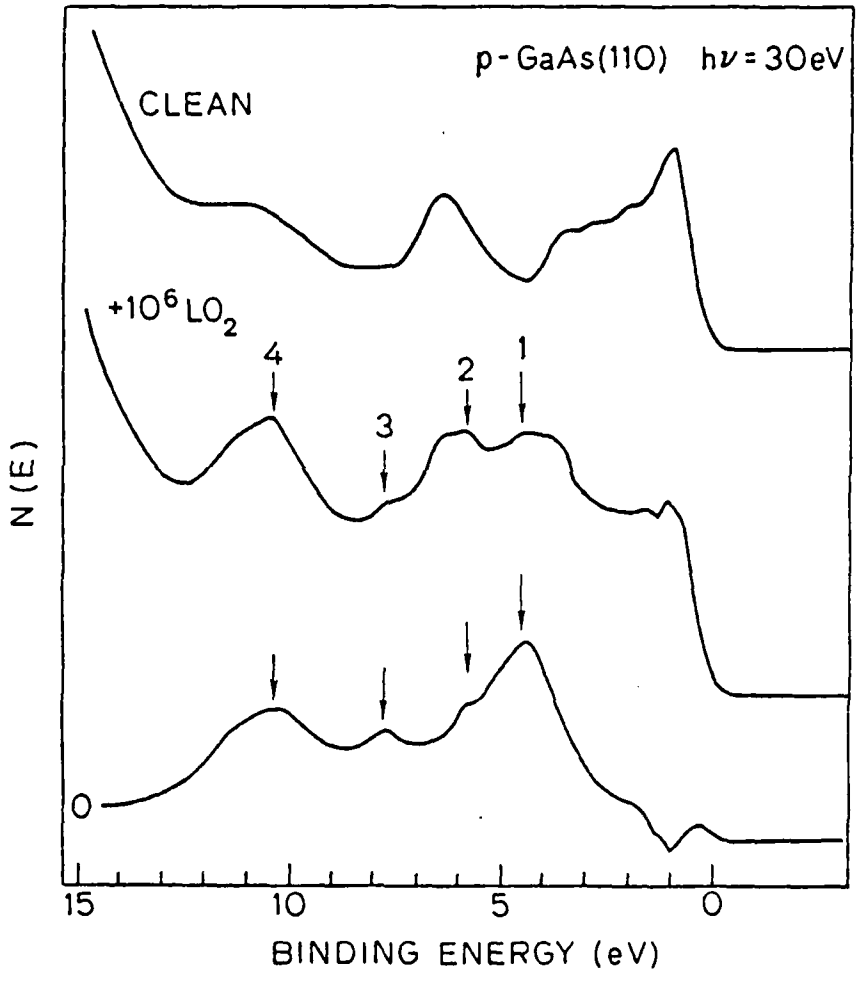
p-GaAs(110) hν = 30eV
CLEAN
+10^6 LO_2
4
3
2
1
0
N(E)
15
10
5
0
BINDING ENERGY (eV)

Chung-yi Su

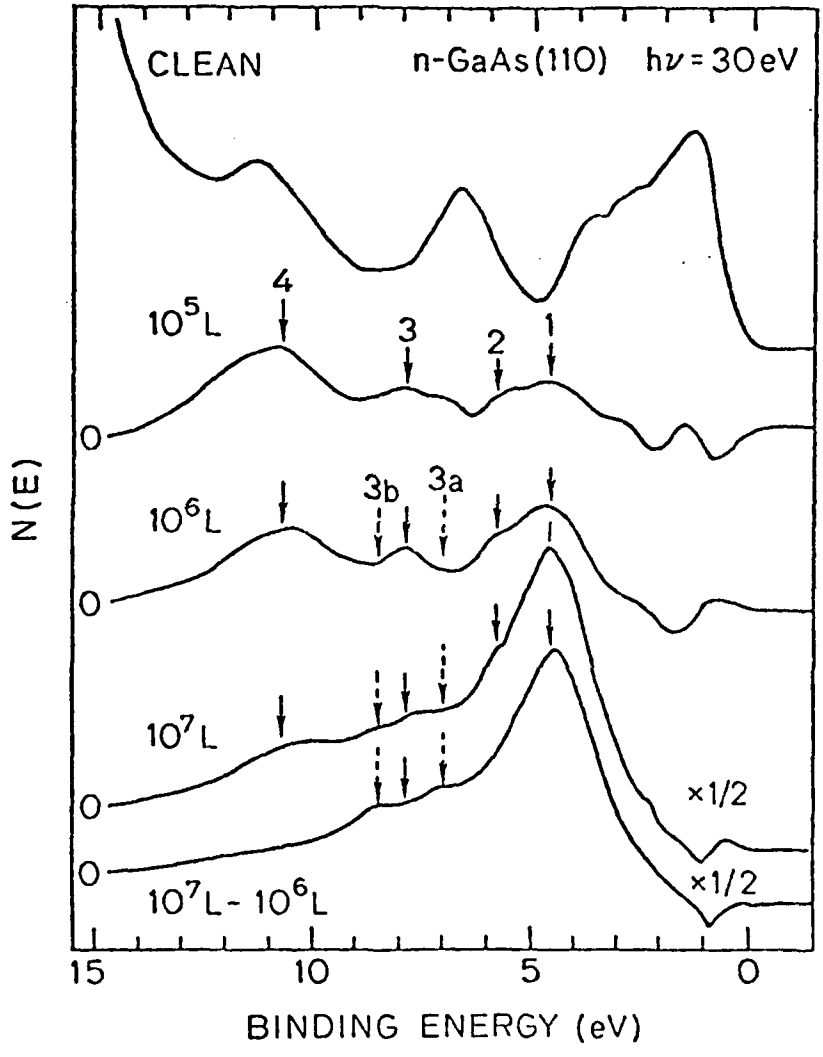
CLEAN
n-GaAs(110) hν = 30eV
10^5 L
4
3
2
1
0
10^6 L
3b
3a
0
10^7 L
0
×1/2
0
10^7 L - 10^6 L
×1/2
N(E)
15
10
5
0
BINDING ENERGY (eV)

Fig. 2

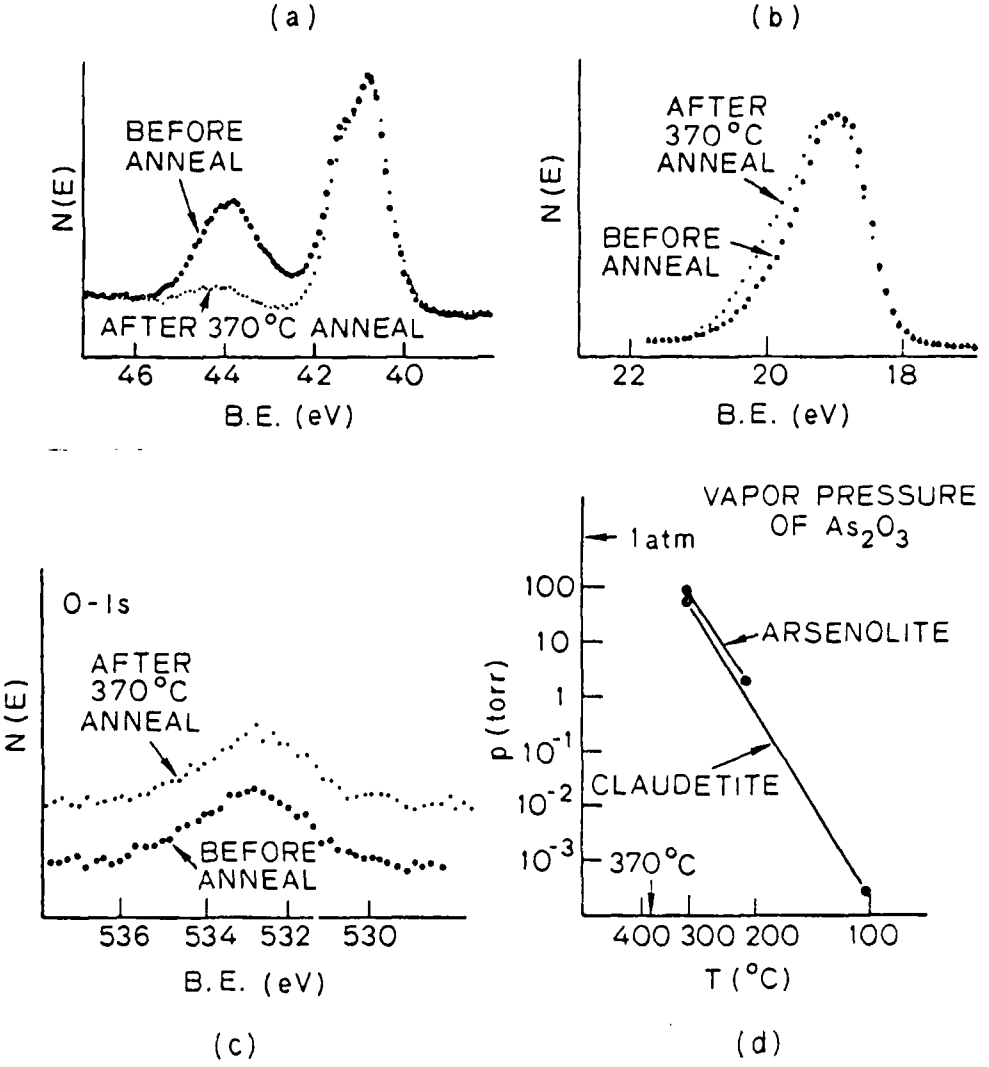
(a)
BEFORE ANNEAL
AFTER 370°C ANNEAL
N(E)
46 44 42 40
B.E. (eV)
(b)
AFTER 370°C ANNEAL
BEFORE ANNEAL
N(E)
22 20 18
B.E. (eV)
O-1s
AFTER 370°C ANNEAL
BEFORE ANNEAL
N(E)
536 534 532 530
B.E. (eV)
(c)
VAPOR PRESSURE OF As_2O_3
1 atm
100
10
1
10^{-1}
10^{-2}
10^{-3}
p (torr)
ARSENOLITE
CLAUDETITE
370°C
400 300 200 100
T (°C)
(d)

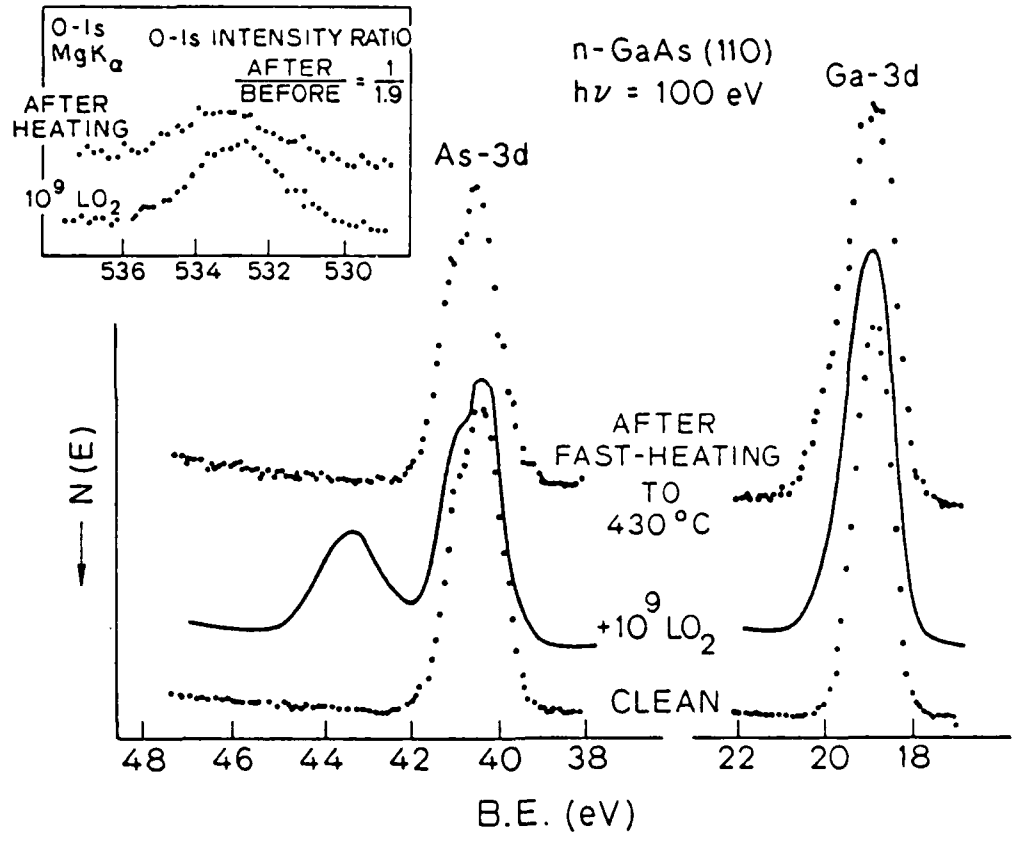
O-1s
MgK$_\alpha$
O-1s INTENSITY RATIO
AFTER / BEFORE = 1 / 1.9
AFTER HEATING
10^9 LO$_2$
536 534 532 530
n-GaAs (110)
hν = 100 eV
As-3d
Ga-3d
AFTER FAST-HEATING TO 430 °C
+10^9 LO$_2$
CLEAN
N(E)
48 46 44 42 40 38
22 20 18
B.E. (eV)

APPENDIX D

In Press - J. Vac. Sci. and Tech. Oct./Nov. 1981

Si-Pd AND Si-Pt INTERFACES

J. N. Miller, S. A. Schwarz,
I. Lindau, and W. E. Spicer
Stanford Electronics Laboratories
Stanford University
Stanford, California 94305, USA

B. De Michelis, I. Abbati,
and L. Braicovich
Istituto di Fisica del Politecnico
Milano, Italy

Abstract

Photoemission (PS) and Auger electron spectroscopy were used to study the formation of Pd silicide in UHV on Si single crystals. The Pd depositions ranged from submonolayer coverages to hundreds of Angstroms thickness. AES sputter depth profiles indicate that room temperature Pd-Si interdiffusion occurs over ~100 Å and that Pd reduces the native Si oxides, with oxygen appearing at the vacuum surface of the evaporated layer. We have been able to separate out the relative contributions of Si and Pd to the silicide valence band by using a wide range of photon energies in the PS studies. The Pd d-bands in the silicide are filled and, due to the strong Pd-Si interaction, are pulled down more than 2 eV relative to Pd metal. In addition, we suggest that the silicide formed at the surface may be more closely related to that of the glassy metals rather than the well-defined (although closely related) Pd_2Si compound. Similar results are also obtained for the system of Pt on Si.

1. Introduction

The transition metal (TM) silicide-silicon interfaces provide an intriguing group of compounds for studyinq the interaction of microscopic solid state chemistry on the macroscopic electrical properties of Schottky barriers [1]. The concept of an abrupt metal semiconductor interface has lost much of its credibility in many material systems [2,3]. Certainly, the very strong electronic interactions and low heats of formation for the silicides make them prime candidates for model systems to study this phenomenon. Pd and Pt silicides have some of the lowest heats of formation of the TM silicides and have been the focus of recent studies [4].

2. *Measurements and Discussion*

The Si samples were prepared by UHV cleavage for the case of the UPS measurements and by cleaved-in air for the AES work. Pd was deposited by vaporizing Pd wire wound on a W filament heater. The thickness of the Pd was monitored using a quartz crystal oscillator, and the amount deposited was controlled from submonolayer up to hundreds of Angstroms.

The AES measurements were performed using a Varian Auger system. The Si was covered with a native oxide estimated to be ~10 Å in thickness as a result of the air cleavage of the sample. As the Pd was deposited on the Si, the peak-to-peak amplitude of the Si, O, Pd peaks were monitored. As increasingly thick Pd layers were deposited, the Pd signal increased as the Si signal decreased. However, the O p-p signal remained the same. Subsequent experiments indicated that the Pd was evaporated without oxygen contamination. After the evaporation and measurements,

an argon ion beam was then turned on and the as deposited interface was sputtered away while a simultaneous record was made of the AES peaks. The corresponding AES depth profile is shown in Fig. 1. At the surface, a significant amount of oxygen and Pd is detected. At increasing sputter times, the oxygen signal quickly disappears and the Si signal begins to increase. The Pd signal also increases with increasing depth for the first 15 Å. Near 20 Å, the signal due to the oxygen vanishes; on the other hand, a significant Pd signal remains to a depth of 140 Å. Pd diffuses very easily through Si, and significant ion knock-on mixing effects must be accounted for when analyzing the sputter profiles. Therefore, the Pd may not be distributed as deep as the sputter profile indicates. However, it is clear that the Pd is mixed into the Si over a considerable distance and not merely an ad-layer on the surface. The driving energy for this strong intermixing comes from the heat of condensation and heat of formation of the Pd-Si alloy. It is also possible to conclude from these experiments that oxygen remains on the surface after Pd deposition is depleted of Si. Perhaps this is due to the characteristics of the thin air oxide and not the general characteristic of Pd-SiO_2 interface. It is clear, however, that not only the intermixing of Pd and Si but also the oxygen removal is of great importance in the formation of ohmic contacts on Si wafers processed in air. Experiments on the native oxide over Si interface on which Au is deposited to Au indicated that the oxide of Si is reduced or dissolved in the Au-Si system [5]. Au, of course, does not form any bulk oxides so that the fact that the oxide disappears from the interface region is somewhat of a surprise from bulk thermodynamic arguments. Alessandrini et al [5] suggest that this is due to the formation of a Au-Si alloy which is first

formed and which then is responsible for the reaction with the thin SiO_2 layer. Bulk thermodynamic arguments also fail to explain why Pd (or Pt) interact with a surface SiO_2. There exists an attractive explanation by analogy to the Au-Si system that an alloy is formed between Si and metal and the resultant alloy can attack the SiO_2.

3. UPS

Aside from its applications in the electronics industry, the Pd-Si interface is of interest for more basic reasons. Palladium silicide is a close relative to a number of unique compounds which are members of the class of glassy metals. These glassy metals possess unique mechanical and corrosion resistant properties and have unique magnetic properties [6].

Pd metal has a valence band about 4 eV wide. The 4d band is partially filled and contains about 9.5 electrons. In the gas phase, Pd will have a d^{10} configuration. So that, a reasonable picture of Pd in the solid state includes a d-band that is almost completely filled with only a small density of empty d-states above E_F.

Si, on the other hand, is a covalent bond semiconductor with a 10 eV band width. From the results discussed in the previous section, we know that the Pd deposited at room temperature mixes with the Si. This can be generalized to suggest that the Pd-Si electronic structure is characterized by strong intermixing rather than a more ideal Schottky-barrier configuration of abrupt metal semiconductor junction.

In the UPS spectra in the low Pd coverage limit, we find what appears to be a broad d-band peak about 3 eV from E_F. Up to a deposition of an equivalent of 6 monolayers of Pd, this d-like peak shifts toward E_F and

stabilizes about 2.5 eV from E_F. Higher coverages of Pd do not change this peak appreciably when the deposition rate is less than 2 Å per second. Annealing this Pd-Si system resulted in no significant change.

In Fig. 2, we present the EDCs obtained for the case of about 6 monolayers of Pd deposited on Si at a photon energy of 40.8 eV. The shape of the EDCs bears a strong resemblance to the density of states of the noble metals: Cu, Ag, Au. However, this resemblance is only fortuitous in certain photon energy ranges.

The density of states (DOS) for the noble metals are characterized by a filled d-like band located a few volts below E_F and a "s-p" band which extends through E_F. This simple model of the DOS of the noble metals is helpful in understanding the macroscopic properties of these materials, such as color and electrical conductivity. It is a little too simplistic a model in that it implies that the d-states are totally decoupled from the s- and p-states. Significant amount of d-state character is mixed into the band states extending to E_F. It seems rather surprising that the d-electron states of Pd could shift to 3 eV greater binding energy when deposited on Si as compared to Pd metal. In the glassy metals formed from Pd-Si, a controversy has arisen over the relative contribution of d-states to the DOS at E_F [8]. In order to gain a greater understanding of the role the d-states of Pd play in the DOS of Pd-Si alloys and confirm that the peaks 2.5 eV below E_F are due to the Pd d-electrons, we will make use of the photon energy dependence of the photoionization cross section. Variation in the photoionization cross section of Pd is responsible for changes in the intensity of the Pd 4d emission between 50 and 200 eV photon energy. In Fig. 3, the photoionization cross section of the Pd valence band measured by Hecht and Lindau [9] is given. At photon

energies above 100 eV, the cross section falls rapidly until it renders a minimum near 130 eV. This minimum corresponds to the Cooper minimum for the Pd 4d levels [10]. Above 140 eV, the curve remains relatively flat. A dashed line is added as a best guess of the relative strength and the monotonic behavior of the cross section for the Si valence band in this energy regime. We first tune $h\nu$ to 80 eV to enhance the Pd contribution to the EDCs; then we tune $h\nu$ close to the Cooper minimum to enhance the Si contribution to the EDCs. Finally, we tune to higher $h\nu$ to show that the Pd contribution tends to increase again. This, of course, makes the implied assumption that the cross section of the constituents can be applied to the Pd-Si alloy. This assumption is readily justified on the grounds that the physical basis for substantial cross-section variation is only modified slightly by the local environment [11].

In Fig. 4, we show the results of these experiments. The EDC at 80 eV looks nearly identical to that taken of 40.8 eV shown in Fig. 2. In the photon energy range 120 to 140 eV, we see new structure appearing in the EDCs which attribute to the Si portion of the DOS. In particular, we note that the emission just below E_F is relatively stronger and even forms a peak at $h\nu$ of 130 eV. The top EDC in Fig. 4 indeed confirms that the Pd 4d intensity returns at higher $h\nu$.

The EDC from the Si (111)-Pt interface is given in Fig. 5. 10 ml of Pt is deposited onto cleaved Si (111). Angle-integrated EDCs were measured with He I radiation ($h\nu$ = 21.2 eV). We also show the EDC from the same quantity of pure Pt deposited onto an inert substrate. As in the case of Pd, evidence is found for the chemical interaction between the silicon and the metal. There is a redistribution of the 5d electrons at the Si+Pt interface which appears to be similar to that found at the

Si (111)+Pd interface. The systematic trends of the electron states in these cases and in other Si d-metal interfaces are discussed in another communication to this conference. Here, it is important to add only one piece of information to that given in Fig. 5. In extensive measurements versus coverage [12], we have found that the EDCs from Si (111)-Pt have the same general shape but that there is a shift of the prominent structure towards E_F when the region is enriched in Pt (i.e., at increasing Pt coverages). Thus, we can say that the "silicide-like" shape of the EDC is due to the formation of an intermixed Si-Pt region with a concentration gradient rather than to the formation of a strictly stoichiometric silicide.

We have obtained the three pieces of information we sought to obtain with this experiment. First, the peaks in the EDCs about 2.5 eV from E_F are indeed due to the 4d levels of Pd in the Pd-Si alloy. Second, a well-defined structure interpreted as due to a Si contribution to the EDCs are visible at $h\nu$ near the Cooper minimum and tend to be obscured at other photon energies. Last, the nature of the emission near the Fermi energy seems to be due to a mix of Si and Pd states. This suggests the d-hybridization at E_F is quite strong.

Acknowledgment

The work at Stanford was supported by the Advanced Research Projects Agency of the Department of Defense and was monitored by the Office of Naval Research under Contract No. N00014-79-C-0072. Part of the experiments were performed at the Stanford Synchrotron Radiation Laboratory which is supported by the National Science Foundation under Grant No. DMR77-27489 in collaboration with the Stanford Linear Accelerator Center and the Department of Energy.

References

1. K. N. Tu and J. W. Mayer, in Thin Films--Interdiffusion and Reactions (edited by J. M. Poate, J. W. Mayer, and K. N. Tu), Wiley, New York, 1978, p. 359.
2. J. M. Andrews and J. C. Phillips, Phys. Rev. Lett. 35, 56 (1975).
3. W. E. Spicer, P. W. Chye, P. R. Skeath, C. Y. Su, and I. Lindau, J. Vac. Sci. Technol. 16, 1423 (1979).
4. J. L. Freeouf, G. W. Rubloff, P. S. Ho, and T. S. Kuan, Phys. Rev. Lett. 43, 1836 (1979).
5. E. I. Alessandrini, D. R. Campbell, and K. N. Tu, J. Appl. Phys. 48, 420 (1977).
6. J. D. Riley, L. Ley, J. Azoulay, and K. Terakura, Phys. Rev. B 20, 776 (1979).
7. G. Busch and H. J. Guntherodt, in Solid State Physics (edited by H. Ehrenreich, F. Seitz, and D. Turnbull), Academic, New York, 1974, Vol. 29, p. 235.
8. M. Muller, H. Beck, and H. J. Guntherodt, Phys. Rev. Lett. 41, 983 (1978).
9. M. Hecht and I. Lindau, private communications.
10. J. W. Cooper, Phys. Rev. 128, 681 (1963).
11. M. S. Banna and D. A. Shirley, J. Electron Spectrosc. 8, 255 (1976).
12. I. Abbati, L. Braicovich, and B. De Michelis, to be published.

Figure Captions

1. An AES sputter profile of Pd deposited on the native oxide covered Si surface. The Si signal is totally depleated from the surface, while the oxygen signal remains at the surface. There appears to be a strong intermixing of the Pd and Si even at room temperature.

2. The energy distribution curve for Pd deposited on the UHV cleaved Si surface at room temperature at 40.8 eV photon energy.

3. The partial photoionization cross section of Pd plotted as a function of photon energy (from Ref. 9). The dashed line is the approximate Si contribution to the EDCs we can deduce from our experiments.

4. Pd deposited on clean cleaved Si surface. Near 80 eV photon energy, the Pd dominates the EDCs. Near the Cooper minimum for the Pd 4d's (120 to 140 eV), the Si contribution to the EDCs becomes stronger. At higher photon energies, the Pd contribution to the EDCs increases as predicted from the cross-section data. The curves have been scaled to be nearly the same size.

5. EDC of 10 ml of Pt deposited on Si (111). The curves were taken at room temperature with He I radiation (21.2 eV).

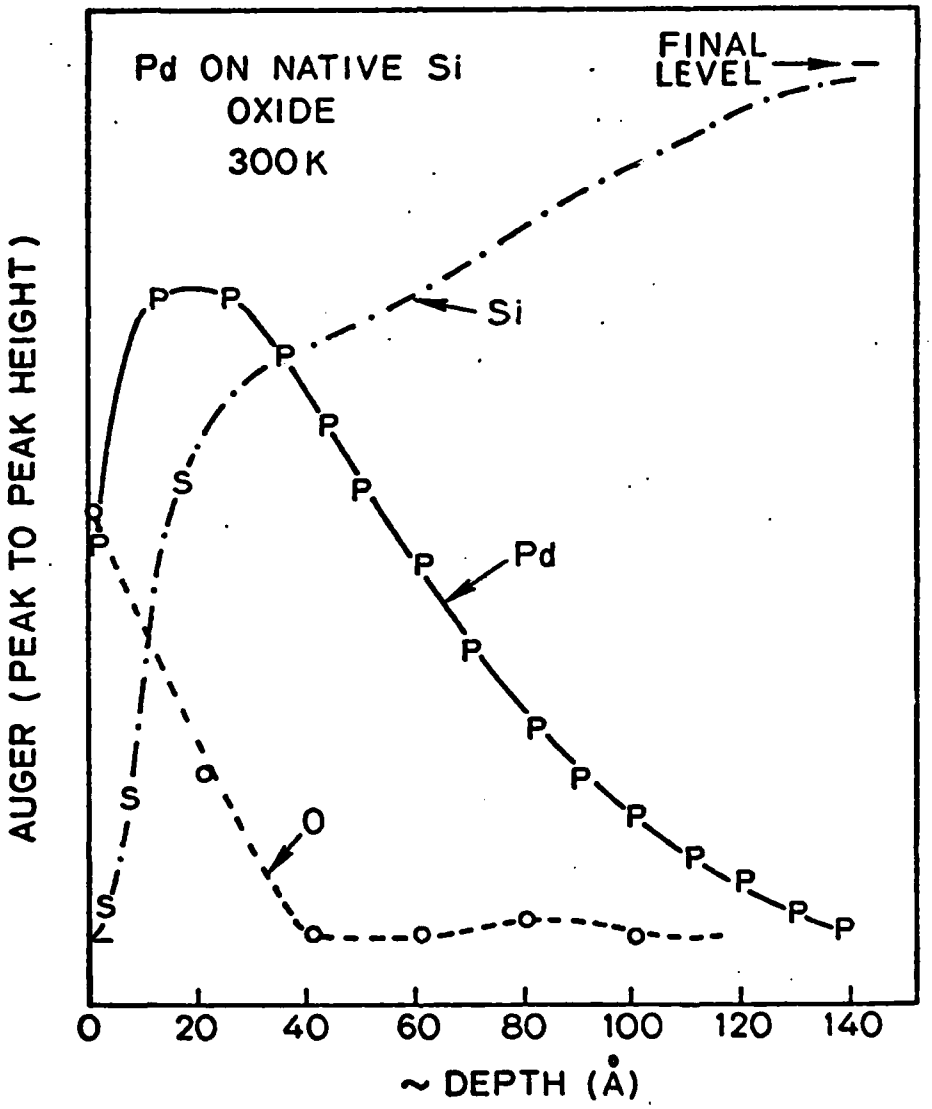
Pd ON NATIVE Si
OXIDE
300K
FINAL LEVEL
Si
Pd
O
S
AUGER (PEAK TO PEAK HEIGHT)
0
20
40
60
80
100
120
140
~ DEPTH (Å)

Fig. 1

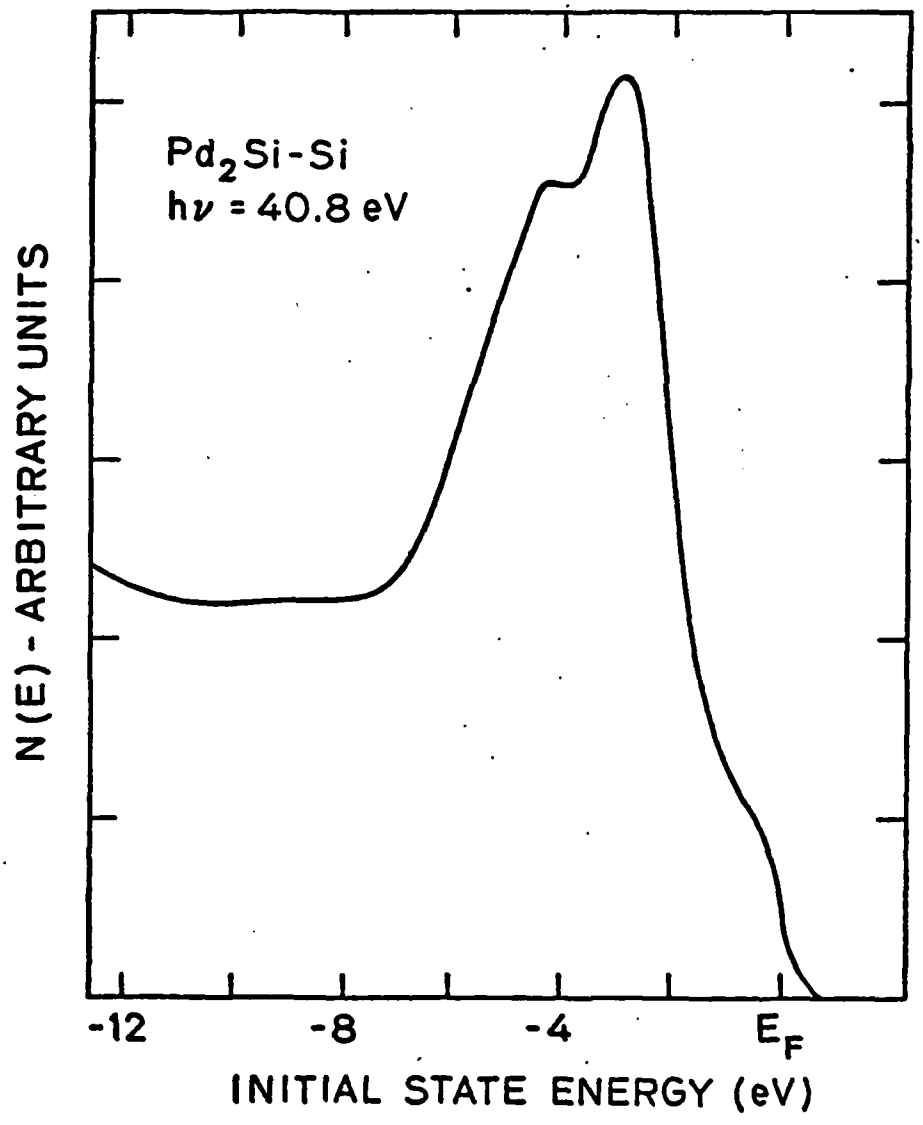
Pd_2Si-Si
$h\nu$ = 40.8 eV
N(E) - ARBITRARY UNITS
-12
-8
-4
E_F
INITIAL STATE ENERGY (eV)

Fig. 2

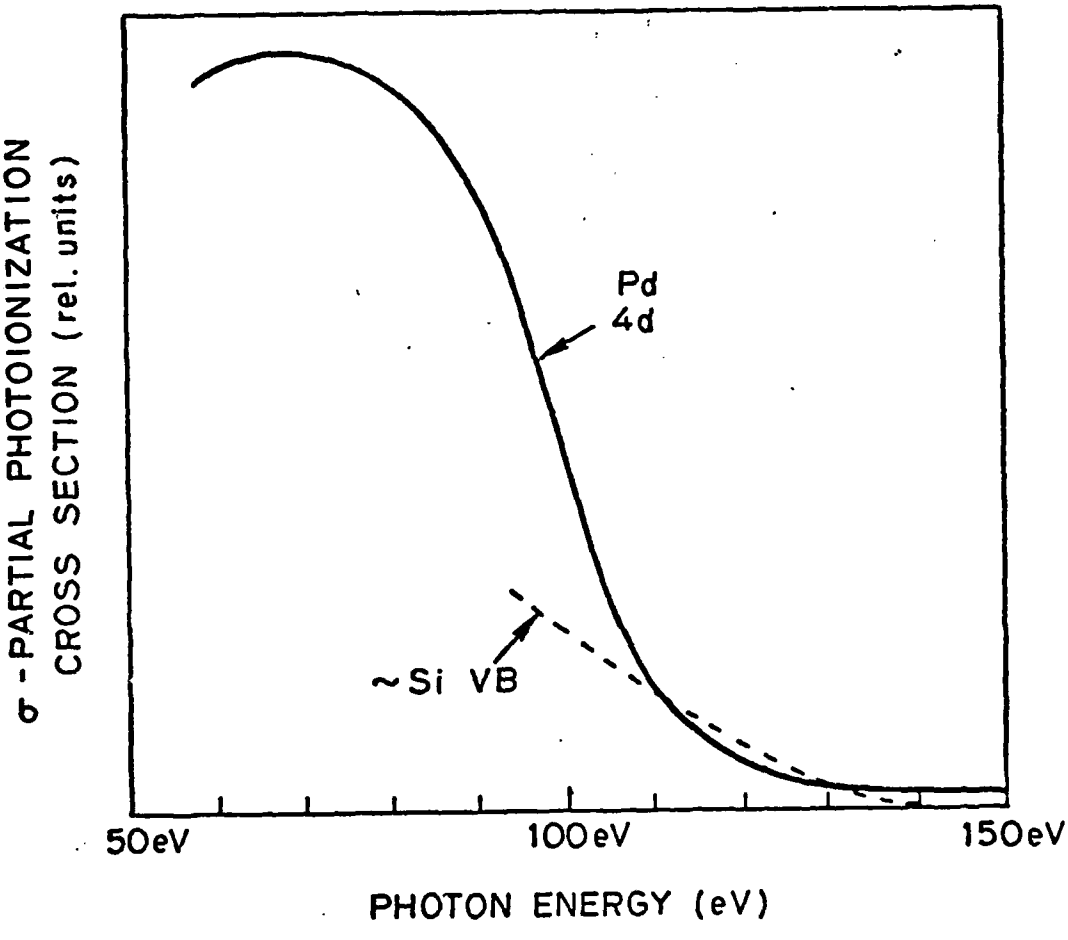
σ -PARTIAL PHOTOIONIZATION
CROSS SECTION (rel. units)
Pd
4d
~Si VB
50eV
100eV
150eV
PHOTON ENERGY (eV)

Fig. 3

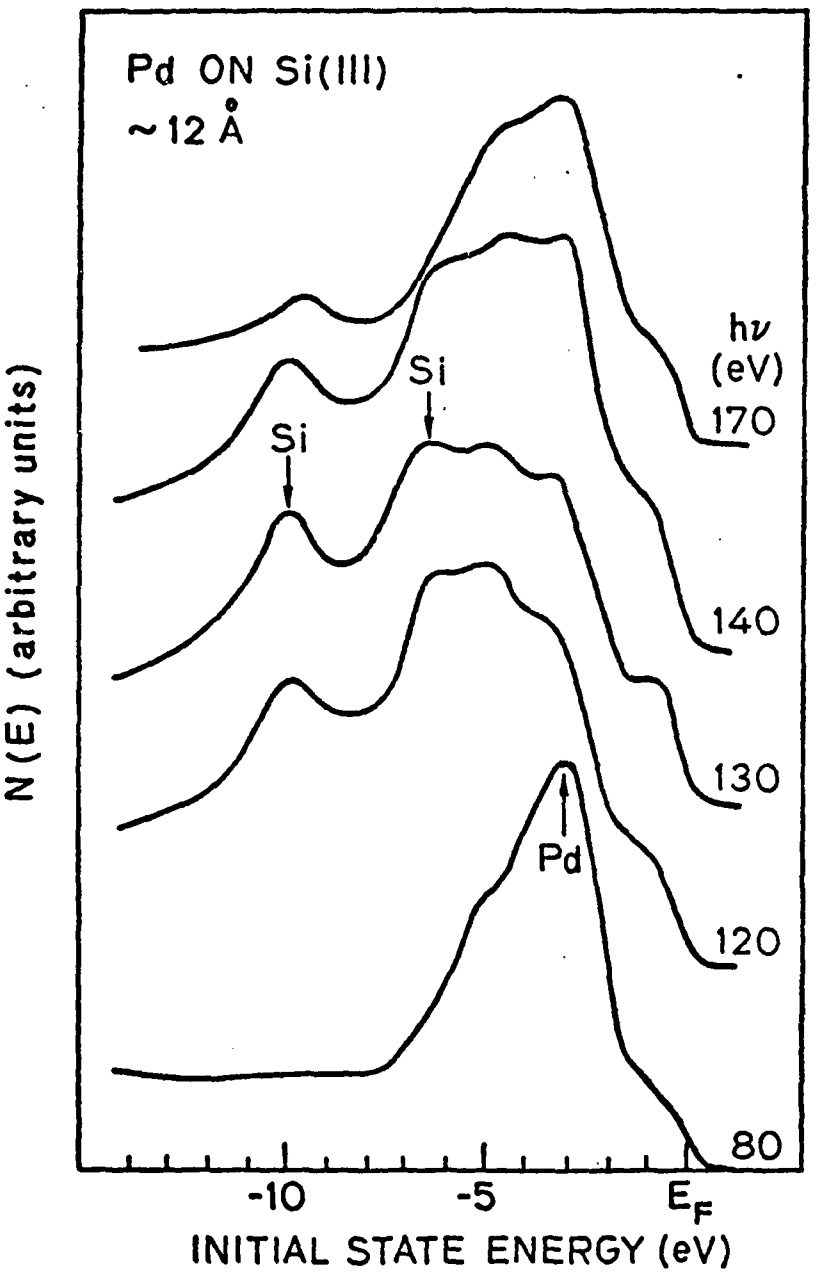
Pd ON Si(111)
~12 Å
hν (eV)
170
140
130
120
80
Si
Si
Pd
N(E) (arbitrary units)
-10
-5
E_F
INITIAL STATE ENERGY (eV)

Fig. 4

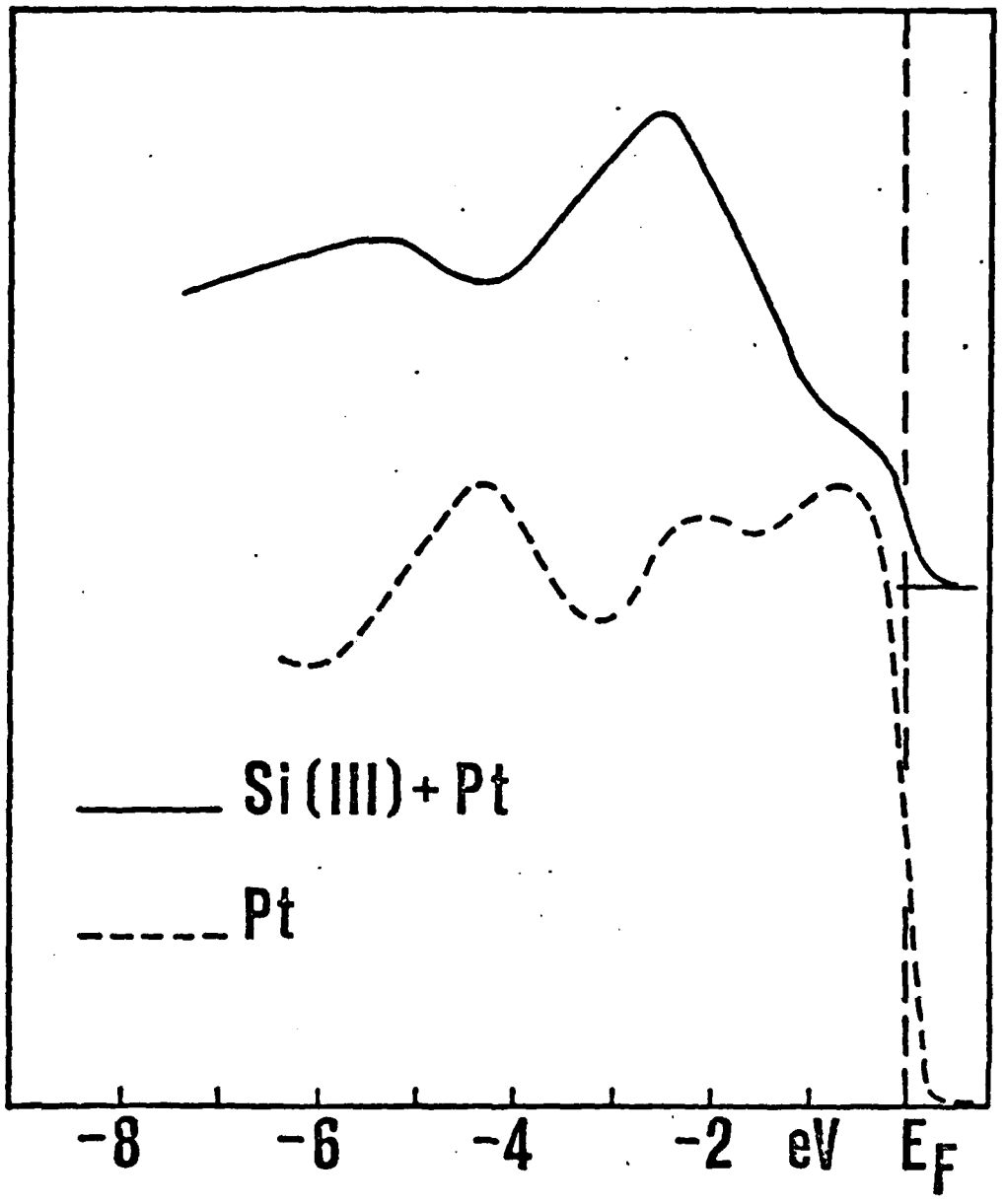

Fig. 5